



Energy, Mines and
Resources Canada

Énergie, Mines et
Ressources Canada

Science and Technology Science et Technologie

580389

Your file Votre référence

Cur file Votre référence

GEOMAGNETIC SERVICE OF CANADA

MAGNETO-TELLURIC PROSPECTING IN THE MOUNT MEAGER
GEOTHERMAL REGION (BRITISH COLUMBIA)
31 pp., 38 figures

Pham Van Ngoc
McGill University
P.O. Box 6079
Postal Station 'A'
Montreal, P.Q.
H3C 3A7

Earth Physics Branch Open File 78-6E
Ottawa, Canada
1978

Price: \$16.00

NOT FOR REPRODUCTION

This document was produced
by scanning the original publication.

Ce document est le produit d'une
numérisation par balayage
de la publication originale.

Earth Physics Branch
1 Observatory Crescent
Ottawa Canada
K1A 0Y3

Direction de la physique du globe
1, place de l'Observatoire
Ottawa Canada
K1A 0Y3

This paper contains 45 per cent
recycled post-consumer fibre Ce papier contient 45 pour cent de
fibres recyclées

EPB
Open File
78-6 (E)

McGILL
UNIVERSITY



ÉCOLE POLYTECHNIQUE
DE MONTRÉAL

INSTITUT DE RECHERCHE EN EXPLORATION MINÉRALE

DEPARTMENT OF ENERGY, MINES & RESOURCES
Earth Physics Branch

MAGNETO-TELLURIC PROSPECTING
IN THE
MOUNT MEAGER GEOTHERMAL REGION
(BRITISH COLUMBIA)

by
PHAM VAN NGOC

February 1978

MINERAL EXPLORATION RESEARCH INSTITUTE

SUMMARY

	<u>Page</u>
ABSTRACT	1
1. INTRODUCTION	4
2. LOCATION OF THE STUDY AREA	5
3. EQUIPMENT AND DATA REDUCTION	6
4. PRESENTATION OF RESULTS.	7
5. GENERAL COMMENTS	10
6. QUALITATIVE INTERPRETATION	11
6.1 Principal directions and apparent resistivity maps at 100 Hz	12
6.2 Principal directions and apparent resistivity at 1 Hz	12
6.3 Pseudo-sections along profile A	13
7. QUANTITATIVE INTERPRETATION	14
7.1 Lower Lillooet Valley zone	14
7.2 Mount Meager, N-NE zone	16
7.3 Mount Meager, S-SE zone	20
7.4 Geoelectrical sections along profiles A and B	22
8. INTERPRETATION AND DISCUSSION	23
9. GENERAL SYNTHESIS OF RESULTS, AND APPLICATION TO GEOTHERMAL POTENTIAL	25
10. CONCLUSIONS AND RECOMMENDATIONS	29
REFERENCES	31

ABSTRACT

The magneto-telluric prospecting program in the Mount Meager area in 1977 included 10 sites supplementary to the 3 sites studied in 1976. The sites are located, along the Lillooet valley to the north of Mount Meager, and along Meager Creek which borders the volcano to the east and south.

The collection of results obtained during the two field seasons allows:

- the establishment of a precise stratigraphy from the superficial cover to the upper mantle, notably in the lower Lillooet valley, where it is clearly confirmed that the crust is thin (average thickness 19 Km) and that the upper mantle is very conductive (resistivity less than 60 Ωm),
- the detection of superficial fracture zones, notably in the Meager Creek hot spring zone,
- the location of conductive zones in the crust, notably in lower Lillooet valley and to the south of the volcano,
- the definition of five deep faults connected with the tectonics of the region as well as with the eruptive mechanism of the volcano, and outlining six structural units in the region under study,

- the definition of the deep structure and electrical properties of the crust and the upper mantle in relation to the recent volcanism and global tectonics.

The new results include other elements in favour of the hypothesis of E.W. expansion of the crust. This expansion would be the origin of the "macroanisotropic" character of the crust and also the existence of an important deep conducting zone in the lower Lillooet valley. This zone, which is located on the NS axis of Cayley volcano, could correspond to a major break in the earth's crust, related to the eruption of the volcano.

To the west of the junction of the Lillooet River and Meager Creek, in the regions neighboring Mount Meager, the rock is clearly less resistant. Faults with major offsets border the zone of eruptions, where the conductive magma can come within 4 Km of the surface in some areas.

In this study area, two regions are defined which present major targets as reservoirs of geothermal energy, and two other zones are considered favourable. Recommendations are put forward for a more detailed study of these areas.

Despite the reconnaissance nature of the two magnetotelluric campaigns, the important data recovered show the applicability of the M.T. method in this type of study. It would be

useful in the future to include M.T. in all studies, either regional or detailed, to evaluate the geothermal energy potential of a region.

1 - INTRODUCTION

Under the terms of an agreement between the Department of Energy, Mines and Resources of Canada, and the Mineral Exploration Research Institute, a magneto-telluric survey was carried out in the Mount Meager geothermal area in the summer of 1977, between June 22 and July 12. This survey is a follow-up to the 1976 reconnaissance survey in the Lillooet valley to the east of Mount Meager, where the magneto-telluric (M.T.) method provided interesting information on the properties of the area from the superficial cover to the base of the crust (PHAM VAN NGOC, 1976). The results of the 1976 survey demonstrated the existence of two levels in the superficial material: a first stratum with a resistivity of about 1000 - 3000 Ωm , and 45-65 m thick, corresponding to gravels, and a second layer with a very low resistivity of 2 - 5 Ωm , 4-5 m thick, which could be either a bed of clay or a layer of volcanic ash. Furthermore, the underlying rock is unusual as it changes from isotropic to anisotropic in its geophysical response from site to site along the Lillooet valley. The major directions of anisotropy being approximately NS and EW. In the valley, the bedrock resistivity in the EW direction is reasonably uniform and in the order of 20,000 Ωm , while the NS direction the resistivity can fall to less than 100 Ωm . To explain these results, we assume the hypothesis that the resistivity lows in the NS direction result from major fracture zones in the crust. The fractures are oriented NS, creating an anisotropic electrical response of the type "macroanisotropy". Finally, the results of the 1976 M.T. survey showed that the crust in the area studied is

relatively thin, with a thickness on the order of 18 to 21 Km, and that it rests on a layer of abnormally high electrical conductivity.

Based on these results it was decided, for the 1977 campaign, to attempt to confirm and study in more details the previous results in the Lillooet Valley, and to extend the study area to the west into the area of Mount Meager, a Quaternary volcano whose last eruption was 2440 years ago, and which numerous studies since 1972 indicate to be a potentially economic source of geothermal power (J.G. SOUTHER, 1975).

2 - LOCATION OF THE STUDY AREA

Ten sites were investigated, along the Lillooet Valley, moving up the valley to the north of Mount Meager, and along Meager Creek to the east and south of the volcano. Figure 1 shows the locations of these sites. Five sites were accessible by road, and are numbered SR1 to SR5, the five others are accessible only by helicopter and are numbered SH1 to SH5. Figure 1 also shows the locations of the three sites of the 1976 survey: the results from these sites will be integrated with the results from the 1977 sites in the final interpretation. Table I gives the NTS coordinates of the total of thirteen sites studied.

TABLE I
 NTS Coordinates of the 13 Survey Sites
 of 1976-77

Site	Longitude	Latitude
SR1	471,400	5,608,200
SR2	474,200	5,605,100
SR3	477,000	5,603,600
SR4	483,500	5,600,400
SR5	486,000	5,600,500
SH1	464,200	5,601,900
SH2	467,200	5,602,400
SH3	460,300	5,615,200
SH4	466,000	5,614,100
SH5	468,800	5,610,900
Site 1(1976)	479,700	5,602,500
Site 2(1976)	488,000	5,599,800
Site 3(1976)	493,500	5,597,400

3 - EQUIPMENT AND DATA REDUCTION

The equipment used for the survey, as well as the method of data reduction are described in an earlier report (PHAM VAN NGOC, 1976) to which the reader is referred for more detailed descriptions. Briefly two types of equipment were used. The magneto-telluric profiling equipment (M.T.P.), TELMAG2, which measures the apparent "scalar" resistivity along the direction of the magneto-telluric line

for 12 separate frequencies from 1 to 2,000 Hz and the magneto-telluric sounding array (M.T.S.) which records simultaneously two telluric components and the two horizontal and orthogonal magnetic components. Data reduction of the recordings allows the definition of the two principal directions and the apparent resistivity tensor designated by ρ_a^{12} and ρ_a^{21} .

4 - PRESENTATION OF RESULTS

Each site is composed of a principal magneto-telluric survey station, and several secondary stations of magneto-telluric profiling to allow extension of the results to higher frequencies, and, to check for the presence of localized anomalies in the area of the principal station. During the 1977 field season, a failure of one of the electronic filters of the TELMAG2, which could not be corrected in the field because of lack of spare parts, prevented the gathering of results for profiling for frequencies greater than 100 Hz. To remedy this lack, the treatment of the data from the soundings is extended as far as possible toward the higher frequencies, up to 500 Hz. These data are complimented by apparent resistivity data and phase angles obtained with the EML6R at 18.6 KHz, from the V.L.F. transmitter at Seattle (Cf. Table II).

TABLE II

Apparent Resistivity and Phase Angle
at 18.6 KHz (V.L.F. Transmitter, Seattle)

Station	Appar. Resist. Ωm	Phase (Degrees)
SR1	1000	59°
SR2	250	48°
SR3	350	55°
SR4	660	51°
SR5	1200	58°
SH1	300	47°
SH2	30	55°
SH3	300	54°
SH4	1000	54°
SH5	300	49°

The V.L.F. apparent resistivity values allow extrapolation of the survey curves to higher frequencies (500 Hz) and allow a good estimate of the thickness and resistivity of overburden. Furthermore, the phase angles, which are all greater than 45°* confirm the presence of a second, more conductive layer under the first resistive layer of overburden.

The profiling data at less than 100 Hz does not add any information of interest to the survey results. Therefore, only the magneto-telluric survey (M.T.S.) results for the ten sites are

* In the M.T. method, a phase angle of 45° corresponds to an electrically homogeneous milieu.

presented here.

Figures 2 to 11 corresponding to the ten M.T.S. stations show the apparent resistivity "tensorial" curves along the two principal directions, and designated respectively ρ_a^{12} and ρ_a^{21} . The principal directions are indicated, on the same figures, by the direction arrows, the solid arrows correspond to ρ_a^{12} and the dotted arrows to ρ_a^{21} . Geographic north (NG) is indicated by an arrow on each orientation diagram. The principal directions are given for only four of the periods studied, since they change very little from one period to another. Since the direction of ρ_a^{12} is nearly NS, and that of ρ_a^{21} is approximately EW, for the discussion that follows we will use the convention that:

$$\rho_a^{12} \approx \rho_a^{NS}$$

$$\rho_a^{21} \approx \rho_a^{EW}$$

It must be recalled, however, that the principal directions are not exactly NS and EW, and that they change from one station to another.

During the season of 1976, the periods studied did not exceed 10 seconds. Consequently the descending limb of the survey diagrams, which indicates the presence of a conductive layer beginning near one second is not completely defined. As a result, if this curve allows definition of the upper boundary of the deep conductive layer with reasonable precision (18 to 21 Km), the value of the resistivity of this layer has been extrapolated (10 Ω m) and its thickness is unknown. During the 1977 field season, the spectrum studied has been widened

toward longer periods as far as 100 seconds. This required longer recording times in the field. Consequently, the parameters of the deep conductive layer have been better defined, as can be determined by examination of diagrams 2 to 11.

5 - GENERAL COMMENTS

Of the ten stations studied, four are located in the bottom of the valley of the Lillooet River, below Meager Creek (Cf. Fig. 1). These stations, SR2, SR3, SR4 and SR5 surround site # 1, studied in 1976, where two soundings were carried out (S1 and S2). It is immediately obvious that their principal apparent resistivity curves show the same features as those obtained in 1976 in the zones of anisotropy, whose existence is clearly confirmed by the new results. To better display the resemblance, on Figures 12 and 13 respectively the curves ρ_a^{21} and ρ_a^{12} corresponding to the four 1977 soundings and the five 1976 soundings have been regrouped. The curves from 1976 are dotted. The different curves of ρ_a^{21} are remarkably similar to one another, indicating the relative uniformity of the electrical properties of the crust in this region along an EW direction. Moreover, the coincidence of the descending branches of the curves indicates that the thickness of the crust is equally uniform, as will be confirmed later, by the quantitative interpretation of the data. Figure 13, corresponding to the NS direction, shows the ρ_a^{12} curves. Although they are not entirely similar, they show the same general features.

Curves SR2, SR3 and SR4 are similar to S1 and S2 of site # 1, while SR5 and S5 (1976, site # 3) situated on either side of the isotropic zone (1976, site # 2) have the same shape.

Ascending the Lillooet Valley above Meager Creek, the curves of surveys SR1, SH5, SH4, and SH3 show a form totally different from that obtained from the curves in the lower valley. They have the same shape as the curves from surveys SH1 and SH2, near the hot springs in Meager Creek south of the volcano. Thus it seems certain that these six surveys are located in an area influenced by the Mount Meager Volcano.

6 - QUALITATIVE INTERPRETATION

The results are examined first from a qualitative viewpoint to delimit the major structural features of the area, before proceeding with the quantitative analysis.

The qualitative interpretation is presented, first of all, as two maps for different frequencies. One, at 100 Hz is used to interpret the superficial features, roughly at the bedrock level, the second at 1 Hz, illustrates the deeper structures. Further qualitative information is presented as pseudosections along profile A, in a NW-SE direction along the Lillooet valley.

6.1 Maps of principal directions and apparent resistivities for the frequency F=100 Hz (Figures 14,15 and 16)

Generally speaking, the map of principal directions at 100 Hz (Cf. Fig. 14) shows that the direction ρ_a^{12} is oriented between N and N30 E, with the direction of ρ_a^{21} orthogonal to it. Aside from local fluctuations, the directions are reasonably uniform. Figures 15 and 16 respectively are the maps of apparent resistivity following the two principal directions. On the map of ρ_a^{12} (NS) (Cf. Fig. 15) the successive zones of anisotropy and isotropy in the lower Lillooet Valley can now be well defined, with the isotropic zone being isolated about sounding S3 (1976 site # 2). In the western area of the map, one can distinguish clearly two zones of differing resistivities separated approximately by the 100 m contour: the area to the N.E. is resistant while the zone to the S.W., corresponding to the core of the volcano, is clearly more conductive. The map of ρ_a^{21} (EW) (Cf. Fig.16) confirms the preceding results, but shows better the western limit of the anisotropic zone of the lower Lillooet Valley, because of the higher EW resistivities in this area.

6.2 Maps of principal directions and apparent resistivities for the frequency F=1 Hz (Figures 17, 18, and 19)

The comments of the previous section apply for these three maps, with the exception of the southern zone of the volcano around

stations SH1 and SH2. In this area, the flow of the contours is completely different for the map of ρ_a^{NS} (Fig. 18) as compared to that for ρ_a^{EW} (Fig. 19). This is interpreted as a change in structural direction of nearly 90° from one station to the other, a change which is clearly visible if one compares the survey curves from these two stations (Cf. Fig. 7 and 8). This observation will be discussed in more details in the section on quantitative interpretation.

6.3 Pseudo-sections along profile A (Fig. 20 and 21)

Two pseudo-sections have been drawn, corresponding to ρ_a^{21} and ρ_a^{12} along profile A between stations SH3 to the N.W. and S5 to the S.E. (Cf. Fig. 37) and based on all the data from stations along the Lillooet River.

The pseudo-section of ρ_a^{21} (Cf. Fig. 20) shows a resistant crust of relatively uniform character in the S.E. part separated from a less resistant crust in the N.W. part by a conductive zone in the area of station SR1. The pseudo-section of ρ_a^{12} (Cf. Fig. 21) allows clear interpretation of the anisotropic properties of the crust in the lower Lillooet Valley, showing the presence of an isotropic block in the area of S3 (between sites 2 and 3 of 1976). Furthermore, one notes a strongly conductive zone, both at the surface, and, at depth, beneath station SR3. This zone could indicate an interesting potential for geothermal power, which will be considered in more details elsewhere in this report.

7 - QUANTITATIVE INTERPRETATION

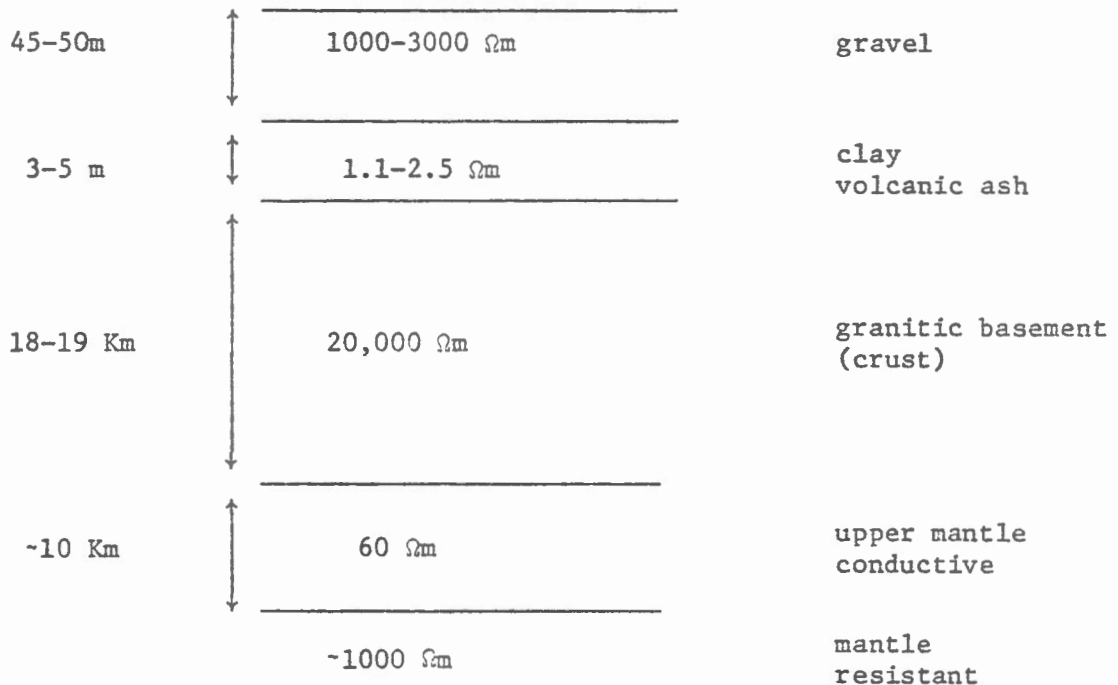
The results from the magneto-telluric study of 1977 indicate that, overall, the region which has been studied is electrically anisotropic. This anisotropy, however, does not have the same origin in the lower Lillooet Valley, above Meager Creek, and in the area round Mount Meager Volcano. In the former case, the phenomenon is one of 'macroanisotropy', and in the latter the anisotropy is the result of lateral electrical discontinuities leaving the region electrically heterogeneous. These discontinuities can correspond to fractures in the cover rocks and in the crust following the volcanic eruptions of Mount Meager. The method of quantitative interpretation adopted depends on the type of anisotropy. In the region under consideration, three different tectonic zones are distinguished by their electrical properties.

7.1 Lower Lillooet Valley zone (Stations SR2, SR3, SR4 and SR5)

As discussed above, the curves of surveys SR2, SR3, SR4 and SR5 confirm the macroanisotropic character of this zone, as was already discovered during the 1976 study (PHAM VAN NGOC, 1976, p.15-16). The interpretation of this type of anisotropy can be based on the hypothesis of tabular structures, using one or the other of the curves for the principal directions. As for the study of 1976, we have chosen to base the quantitative interpretation of the $\rho_a^{21}(EW)$ curves which

yield a better estimate of the thickness of the earth's crust, since in this direction the resistivity contrasts are largest. Figures 22-25 show the results of the interpretation for the four new stations in the lower Lillooet Valley.

The same orders of magnitude as were found in 1976 are given by the present survey, but the estimates are better for the deep conductive layer because of the recordings at longer periods. The typical geoelectrical section for the lower Lillooet Valley is:



Because of lack of data at the longer periods, the resistivity of the deep conducting layer was perhaps slightly underestimated in 1976 (10 Ωm). It is confirmed, however, that the resistivity of this layer is low, even at 60 Ωm , and that the hypothesis that the base of

the crust is at an unusually elevated temperature, which combined with a state of hydration has led to the presence of a partial melt in the area, is still viable.

In the quantitative interpretation which follows, the depth of the top of the deep conductive layer (the upper mantle) has been estimated with good precision, on the order of 10%, its thickness (10 Km) as well as the resistivity of the underlying layer (1000 Ωm) however, are estimated only by extrapolation of the last parts of the survey curves.

7.2 The zone North and Northeast of the Mount Meager Volcano (Stations SR1, SH5, SH4 and SH3).

Examination of the maps of apparent resistivity at 100 Hz (Figs. 15 and 16) and at 1 Hz (Figs. 17 & 18) shows clearly the existence of an important feature in the direction N.W.-S.E., a feature especially visible on the map of $\rho_a^{12}(\text{NS})$ at 1 Hz (Cf. Fig. 18) as in this zone ρ_a^{12} corresponds to the transverse direction. It is known that magneto-telluric transverse apparent resistivities tend to show a strong contrast associated with electrical discontinuities. In this case the discontinuity corresponds to a major feature probably affecting the entire thickness of the crust. Its trace at depth probably corresponds to the 1000 Ωm contour line on figure 18. This feature can be attributed to a major break or fault along the northeast flank of the volcano, and associated with its eruption. The orientation of this

fault is also well indicated by the strong inclination of the principal direction ρ_a^{21} at station SH4 at 1 Hz (Cf. Fig. 17). It is of interest to note that, in an unpublished article, kindly communicated by the authors, T.J. LEWIS and J.G. SOUTHER (1978) indicate the presence of a fault near the hot spring of Pebble Creek (Figure 2 of their article).

In this case, studying a heterogeneous structure, the tabular hypothesis for quantitative interpretation risks being in error. Rigorously, more complex calculations are required, notably those considering the effect of two-dimensional structures. Aside from being long and laborious, these calculations are not justified unless sufficient data are available to formulate good models for calculation.

In a case such as the present, the most practical method is to choose the apparent resistivity curve which shows the least influence of lateral electrical discontinuities, and to interpret this curve using a pseudo-tabular hypothesis. In this approach it is necessary to effect a theoretical study of a typical case involving a two-dimensional structure. Consider a cylindrical structure of rectangular section and of low resistivity (10 Ωm) embedded in more resistant surroundings (1000 Ωm). Figure 26 shows the model curves along the two principal directions, corresponding to a station vertically above and centered on the conducting structure (station A of Figure 26). The same figure shows the form of the survey curve based on the tabular hypothesis. It can be seen that although for the shorter periods the three curves are sensibly the same, for the long periods the curve E (longitudinal resistivity) and curve H (transverse resistivity) diverge strongly. The impression is that curve H, descending regularly, is essentially controlled by the conductive structure, even for very long periods.

On the other hand, curve E climbs sooner because of the influence of deeper resistant layers, and even too quickly compared to the tabular curve. Of the two curves, however, curve E shows the better resemblance to the tabular curve, and is the curve to be chosen for study based on the pseudo-tabular hypothesis. It ought to be noticed, however, that the descending parts of curve E and the tabular curve are very close, and it follows that the estimate of the depth of the top of the conducting structure will not be very much in error. On the other hand, the resistivity of the layer is overestimated and its thickness underestimated because of the divergence of curve E from the curve of the tabular case.

Continuing with the same structure, but placing the station external to the conductive zone (station C of Fig. 27), the bedrock under station C is now resistant and homogeneous. The model curves of Figure 27 show that curve H, unlike the preceding case, reliably reproduces the homogeneous character of the bedrock, and allows a correct estimate of its resistivity. Curve E, on the other hand, still shows the influence of the conductive structure for short periods.

The study of the foregoing theoretical case allows the correct choice of survey curves for the quantitative interpretation of stations SH3, SH4 and SH5. The buried conductive structure could in fact correspond to the magma chamber of the volcano, bordered, in this area, by the N.W.-S.E. fault already discussed. Station SH3, situated to the south of the fault, is located in the conductive zone, and corresponds to the case of station A in the theoretical example. SH4 and SH5, located north of the fault, correspond to station C in

the theoretical example. Thus, for the reasons discussed above, the quantitative interpretation is based on:

- curve ρ_a^{21} (EW) for SH3
- curve ρ_a^{12} (NS) for SH4 and SH5

The results of this interpretation are shown on Figures 28, 29 and 30. These results confirm the importance of the major feature already discussed. If the depth of the deep conducting layer under SH4 and SH5 is in the order of 17-18 Km, it climbs to 9 Km under SH3, a change in depth of 8 Km (Cf. Fig. 36). Note that the results indicated here are only approximate, since the interpretation based on the pseudo-tabular hypothesis is not rigorously correct. However, as discussed above, the estimate of the depth to the top of the conductive layer is reasonably good, except perhaps for station SH3 (Cf. Fig. 28) for which the resistivity of the deep conductive layer (layer 4) should be lower (less than 15 Ωm), and the thickness greater (larger than 7 Km). These uncertainties aside, it seems undeniable that there is a major magma body under the volcano to the south of the N.W.-S.E. fault.

The interpretation of station SR1 is also problematical. The station is located at the intersection of the fault previously discussed with another N.S. fault which borders the volcano on the east, and separates it from the anisotropic zone of the lower Lillooet valley. Here again the case cannot be treated by either a two-dimensional or a tabular model. In this case the quantitative interpretation is nearly impossible. However, it seems that the influence of the N.S. fault dominates at this station (Cf. Fig. 16 and 19). Thus the curve ρ_a^{12} (NS) has been used for the quantitative interpretation of

station SRL (Cf. Fig. 31). The results, however, must be viewed with caution, and ought not to be considered more than order-of-magnitude estimates. With the foregoing reservations, we can once again discern a major change in depth of the magma chamber, for the top of the conductive zone rises to 8 Km. Furthermore, the crust is strongly fractured above the magma chamber, since its resistivity is lowered to 500 Ωm .

7.3 The zone south and southeast of the Mount Meager Volcano (stations SH1 and SH2)

Comparing the sounding curves from stations SH1 and SH2 (Cf. Figs. 7 and 8 respectively) it is immediately evident that the apparent resistivity values ρ_a^{12} and ρ_a^{21} are nearly reversed going from one station to the other. Moreover, there is a general lowering of the values of ρ_a^{12} and ρ_a^{21} towards the short periods for these two stations with respect to the other ones. Since we are in the zone of emergence of the hot springs of Meager Creek, it may be expected that the superficial resistivities should be somewhat lowered. This is confirmed by stations SH1 and SH2, which also show the presence of a strong electrical anisotropy. This latter feature can be explained by the presence of a wide fracture zone in the bedrock.

To explain this, consider another theoretical case of a conducting trench-like structure, infinitely long, in a resistant bedrock (resistivity 1000 Ωm), the conducting trench having the same resistivity as the overburden (10 Ωm) (Cf. Fig. 32). The results of the theoretical

calculations show that the survey curves for the two principal directions, for station A placed vertically over the conducting trench, continue to diverge even for very long periods. The effect is that curve H (transverse resistivity) remains dominated by the conducting trench, and does not reveal the effect of deeper layers. Curve E (longitudinal resistivity) on the other hand, stays relatively close to the tabular model curve. It seems fairly clear that SH1 is influenced by a fracture zone oriented E.W. (in the direction of ρ_a^{21}) since the ρ_a^{12} curve shows low values even for long periods. The same phenomenon can be observed at station SH2, but here the fracture zone is oriented NS, (in the direction of ρ_a^{12}). Thus, following the logic of an earlier section, the quantitative interpretation is based on curve ρ_a^{21} for station SH1 and on curve ρ_a^{12} for station SH2. Figures 33 and 34 show the results obtained for these stations. Here once again the interpretation based on the pseudo-tabular hypothesis is not rigorously correct. However, the results confirm with good precision the pronounced rise in the magma chamber, with the top at a depth of 4 Km under SH2. Furthermore, this last station's results indicate the presence of a very thin and conductive overburden, composed of a superficial layer of 12 m thickness and 100 Ωm resistivity, followed by an extremely conductive layer whose resistivity is as low as 0.4 Ωm . Station SH2 is placed at a hot spring, and drilling at this location has shown the presence of a layer of hot water at 59°C, under a cover of 10 m of gravel (LEWIS, T.J. and SOUTHER, J.G., 1978).

7.4 Geoelectrical sections along a N.W. profile (profile A) and along a N.S. profile (profile B)

To better illustrate the deep structure and tectonics of the study area, the results of the quantitative interpretation, already discussed, are presented as two geoelectrical sections corresponding to two profiles: profile A in a N.W.-S.E. direction, the same profile as in the pseudo-sections of Figures 20 and 21, and profile B in a N.S. direction between the two extreme stations SH4 and SH1 (Cf. Fig. 37).

Figures 35 and 36 show respectively geoelectrical sections A and B. For each of these profiles, two sections have been drawn corresponding to two different depth scales. This allows better resolution of the structure of the overburden, and the deep crustal structure. Under each station, the numbers give the resistivities in Ωm for the different layers. Stations having a circle around the station number are those for which the quantitative interpretation was based on ρ_a^{12} . For the other stations curves ρ_a^{21} have been retained, for the reasons discussed above.

It can be seen that the earth's crust in the study area is highly resistant (20,000 Ωm), and of reasonably uniform thickness, in the order of 17 to 21 Km, with the exception of the fault zones in the immediate area of Mount Meager. Profile A, (Cf. Fig. 35) however, shows a less resistant crust (8,000 Ωm) in the northern sector of Mount Meager (stations SH3, SH4 and SH5). It is probably the same case for the entire area of the volcano, as shown by profile B (Cf. Fig. 36) where the resistivity of the crust overlying the magma

chamber is 6,000 Ωm and 600 Ωm respectively under SH2 and SH1. The crust under SH1 is strongly fractured as a result of the eruption of the volcano. The situation is that of a wide fracture zone affecting the entire thickness of the crust, and bordered on the east by a NS fault situated somewhere between stations SH1 and SH2. The structural complexity of this zone makes the quantitative interpretation difficult. The situation is similar for stations SH3 and SR1 which lie in the strongly perturbed zone to the north. The question marks (?) on the sections as well as the dotted horizons reflect the uncertainty in the depth determinations.

Finally it should be noted that under stations SH4 and SH5, to the north of the N.W.-S.E. fault, there is a layer of conducting material whose resistivity is more (350 Ωm under SH5 and 600 Ωm under SH4) than the conductive material of resistivity 60 Ωm under all the other stations. Do these results indicate the presence of another type of upper mantle material to the north of the N.W.-S.E. fault? The problem is not yet resolved.

8 - INTERPRETATION AND DISCUSSION

In the preceding paragraph, the interpretation was carried out to obtain quantitative information, as exactly as possible, on the deep structure of the earth's crust. The interpretation was based on the choice of the tensor apparent resistivity curves which showed the least influence of superficial structures.

In this section, the tensor apparent resistivity curve which was not selected for quantitative interpretation is re-examined to complement the interpretation, particularly in an effort to define further conductive zones in the crust, which could correspond to reservoirs of geothermal power. The existence of a conductive layer is indicated by the downward inflexion of the apparent resistivity curve. The depth to the top of the layer can be estimated by supposing that the layer is infinitely conductive and using the descending limb of the survey curve.

Examination of the principal apparent resistivity curves not yet interpreted which show one or more descending limbs due neither to superficial effects nor to lateral effects has allowed the definition, for supplementary interpretation, of two groups of curves:

- the ρ_a^{12} (NS) curves for stations in the lower Lillooet Valley,
- the ρ_a^{12} (NS) curve for station SH1.

The curves ρ_a^{12} (NS) of the first group have already been grouped in Figure 13, where two descending limbs can be clearly distinguished. These two limbs correspond to two conductive zones, indicated on the figure by C1 and C2. The following table gives the estimates of the depths to the tops of the conducting zones:

Stations	Layer C1	Layer C2
SR2	500 m	3.4 Km
SR3	260 m	1.7 Km
S 1	500 m	3.4 Km
SR4		3.4 Km
SR5		3.4 Km

The positions of these zones is indicated on Figure 35. The curve ρ_a^{12} (NS) for SH1 shows a descending limb for the very long periods which may be attributed to the presence of a conducting layer C3 (Cf. Fig. 2). The presence of this layer, however, is not clearly confirmed, as in the preceding case, for neighboring stations, and furthermore SH1 is located in a structurally very complex area. However, magneto-tellurically speaking, the existence of C3 is indicated, and the depth to the top of this structure is estimated at 1.6 Km, and the zone is shown on Figure 36.

It is also to be noted that there may be two other conducting zones, one under station SR1, the other under SH3. Their existence, however, is indicated only by very slight inflection of the curves to the very short periods (Cf. Figs. 2 and 9) and further field measures would be necessary to confirm these zones sufficiently to consider them.

9 - GENERAL SYNTHESIS OF THE RESULTS AND APPLICATIONS TO GEOHERMAL POTENTIAL

The body of results considered in the foregoing sections is summarized on Figure 37. The figure shows the major faults which affect the deep crustal structure. These faults, five in number, (F1, F2, F3, F4 and F5) outline six structural units in the study. These units are, from East to West:

1. Anisotropic zone of Lillooet Valley

This zone was discovered during the field season of 1976, at site # 3 (station S5). No follow-up work was done during the 1977 field season.

2. Isotropic zone of the lower Lillooet Valley

This zone is now considered to be an exceptional case in the area, and well defined in space (Cf. the pseudo-section of Fig. 21), since the general population of rock in the area is generally anisotropic, and has undergone major tectonic movements.

3. Second anisotropic zone of the lower Lillooet Valley

The hypothesis formulated in the first report (PHAM VAN NGOC, 1976), that the opening of a N.S. rift system is responsible for the opening of the subvertical fracture zones in the N.S. direction, which produced in the earth's crust a state of electrical 'macro-anisotropy' was fully confirmed during the present study. Furthermore, the supplementary stations measured in 1977 have allowed the definition, within the wide zone of anisotropy, a relatively more conductive zone localized beneath station SR3 (Cf. Fig. 21). The existence of this latter zone, as well as that of the two layers C1 and C2 in the same site, are another confirmation of the preceding hypothesis. Finally, Figure 38 which reproduces a section of the geological map of the Pemberton area (92J) not yet published, compiled by G.J. Woodsworth (1977), of which we have just received a copy, indicates that the zone of anisotropy is located exactly along the prolongation to the north of another recognized Quaternary volcano, Mount Cayley. More exactly, if the surface expressions of the Garibaldi volcanic group, aged

Pliocene to Recent (stratigraphic series 21 of the geological map) are joined by a straight line, the line passes exactly through station SR3 in the Lillooet Valley. These features lead us to believe that the crustal expansion associated with the opening of a rift system has caused a major break in the crust, in the NS direction, along the line joining the Cayley volcano and station SR3. In association with this hypothesis, the conductive zone located under station SR3 is an interesting target for geothermal exploration, and merits further study. In the same vein, the aligned outcrops of rocks of the Garibaldi group to the south of Mount Meager in the Elaho Valley mark the location of another major crustal NS fracture, which intersects the southern limit of the Meager volcano in the C3 conductive zone of station SH1.

4. The zone north of Mount Meager

The electrical properties of the crust in this area were discussed in a previous section. The presence of hot springs in Pebble Creek can be linked to the fault F4 limiting the southern extension of the zone. No important conducting layer has been observed in the interior of the block, with the eventual exception of a zone located under SH3 (Cf. end of section 8). The geothermal potential of this zone should be re-evaluated by complementary studies.

5. Upper Meager Creek valley zone

The area is characterized by the presence of a superficial fracture zone running E.W. along Meager Creek, and by another conductive zone, layer C3, running N.S. at depth. Further, the block is more conductive than the other blocks, and the magma chamber is probably relatively close. This is a zone of geothermal interest, since as

well it is located in the extension of a possible crustal fracture coming from the Elaho Valley, a fracture associated with the eruption of Mount Meager.

6. Lower Meager Creek valley zone

This zone is separated from the preceding zone by the fault F5, and is characterized by a superficial fracture zone, but of orientation N.S. It is this fracture zone which gives access to the surface to the series of hot springs running along the lower valley of Meager Creek. The block is more resistant than zone 5, but the magma chamber seems to mount quite close to the surface (4 Km).

Further north, a strongly tectonized zone under station SR1 could offer a certain geothermal interest. However, zones 4 and 5 should be studied in more details to better determine their deep structure.

In summary, from the point of view of electrical properties, the rocks of the study region show a generally anisotropic character, with the exception of a small zone located near North Creek in the lower Lillooet Valley. The anisotropy is the result either of tension in the earth's crust following an E.W. expansion in the area, or of multiple fractures in the granitic portion of the crust or in the superficial cover material following explosive eruption of the volcano as shown by the geological studies in the area (T.J. LEWIS and J.G. SOUTHER, 1978).

10 - CONCLUSIONS AND RECOMMENDATIONS

The collection of results obtained during the two magnetotelluric surveys of 1976 and 1977 demonstrates the confidence that may be placed in the results, as well as the potential of the M.T. method in structural studies both of superficial and deep features. Even with the limited number of stations studied in the Mount Meager area, the M.T. method has been shown capable of defining, on the one hand, the major features of regional tectonics, to the base of the earth's crust, and on the other hand of locating small-scale superficial features which could present geothermal targets.

The campaigns carried out to date, however, are of a reconnaissance and developmental nature. M.T. results are extremely informative and their interpretation can be carried much farther, notably with two-dimensional models, if enough stations are established in the field following a sensible program of data acquisition. For future studies, we recommend two types of data acquisition programs:

1. A reconnaissance campaign in other regions, such as the Squamish Valley near Mount Cayley and the Elaho Valley, to confirm the existence and extent of the two major crustal fault zones which are related to Mount Meager and Mount Cayley.
2. Detailed prospecting in the potentially interesting zones already defined by the reconnaissance surveys. These detailed campaigns should be organized at the industrial scale, with appropriate support, since the station density should be sufficient (with a survey station

every kilometer or every 500 meters, for example) to provide as precise a quantitative interpretation as possible. Thus for the Mount Meager area, we recommend a detailed study of the following zones (in order of decreasing interest) based on the initial magnetotelluric results:

- . zone SH1 : detail the layer C3 and fault F5
- . zone SR3 : interpret more precisely layers C1 and C2
- . zone SR1 : confirm the presence of a conducting layer
in the block
- . zone SR3 : idem.

These are the zones which are likely to contain reservoirs of geothermal energy between 300 m and 2 Km.

We consider that even at industrial scale, the M.T. method is a most effective geophysical method. It is necessary, however, that the method be applied in a suitable manner with proper support, and a thorough theoretical knowledge of the problem under study.

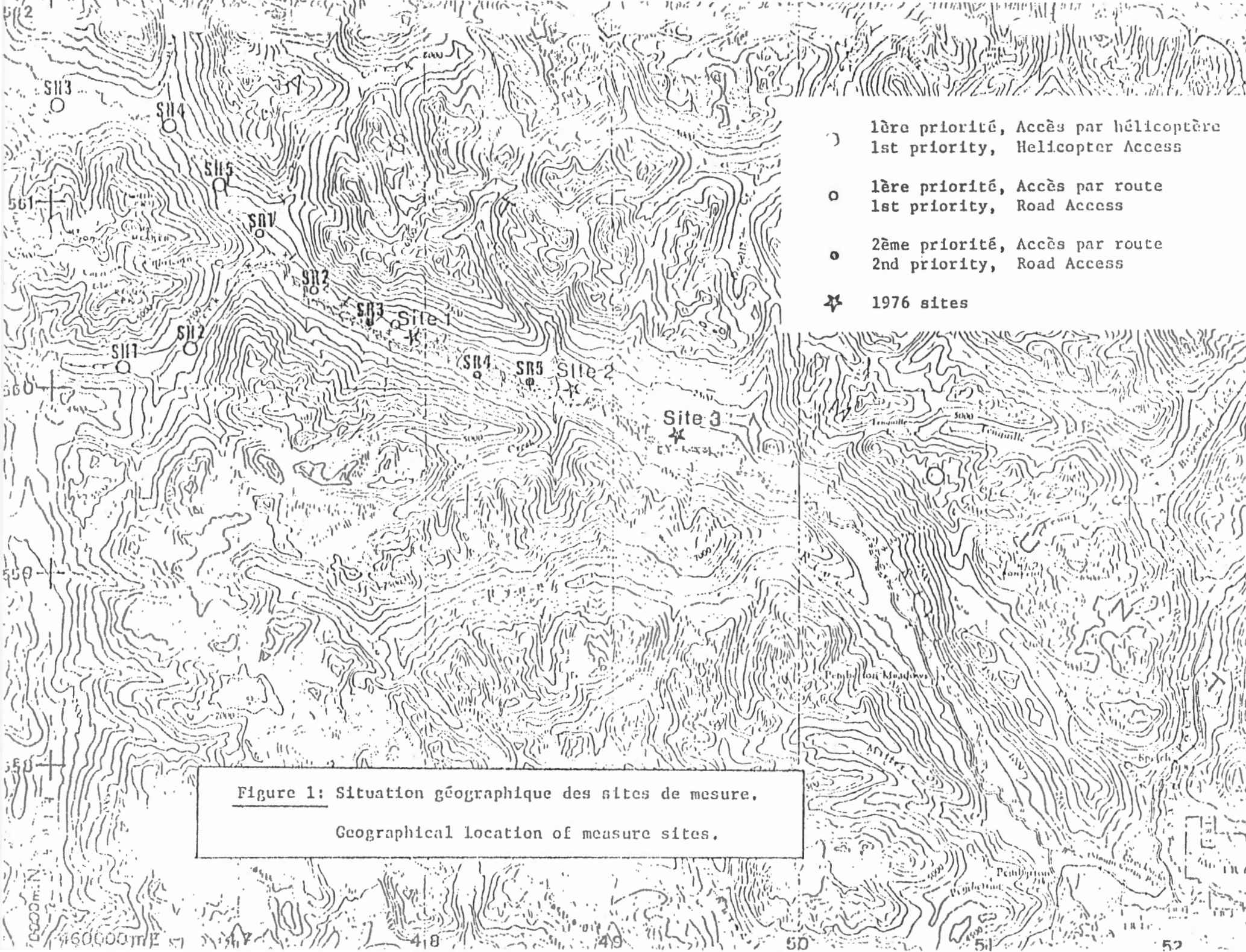
Montreal, 8th February 1978

PHAM VAN NGOC
Ing. Géophys., Doct.ès Sc.

PVN/rr

REFERENCES

- LEWIS, T.J. et SOUTHER, J.G. (1978). Meager Mountain, B.C.,
a possible geothermal resource.
DEMR, Geothermal Series, N^o 9.
- PHAM VAN NGOC (1976). Reconnaissance magnéto-tellurique dans
la vallée de Lillooet (Colombie Britannique).
Rapport IREM-EMR, Départ. Phys. du Globe, Ottawa.
- SOUTHER, J.G. (1975). Geothermal Potential of Western Canada.
Dans Proceedings, Second United Nations Symposium on
the Development and Use of Geothermal Resources,
Vol. 1, p. 259-267.



- 1ère priorité, Accès par hélicoptère
1st priority, Helicopter Access
- 1ère priorité, Accès par route
1st priority, Road Access
- 2ème priorité, Accès par route
2nd priority, Road Access
- ★ 1976 sites

Figure 1: Situation géographique des sites de mesure.
Geographical location of measure sites.

P_a (3.2 m)

STATION SR.1

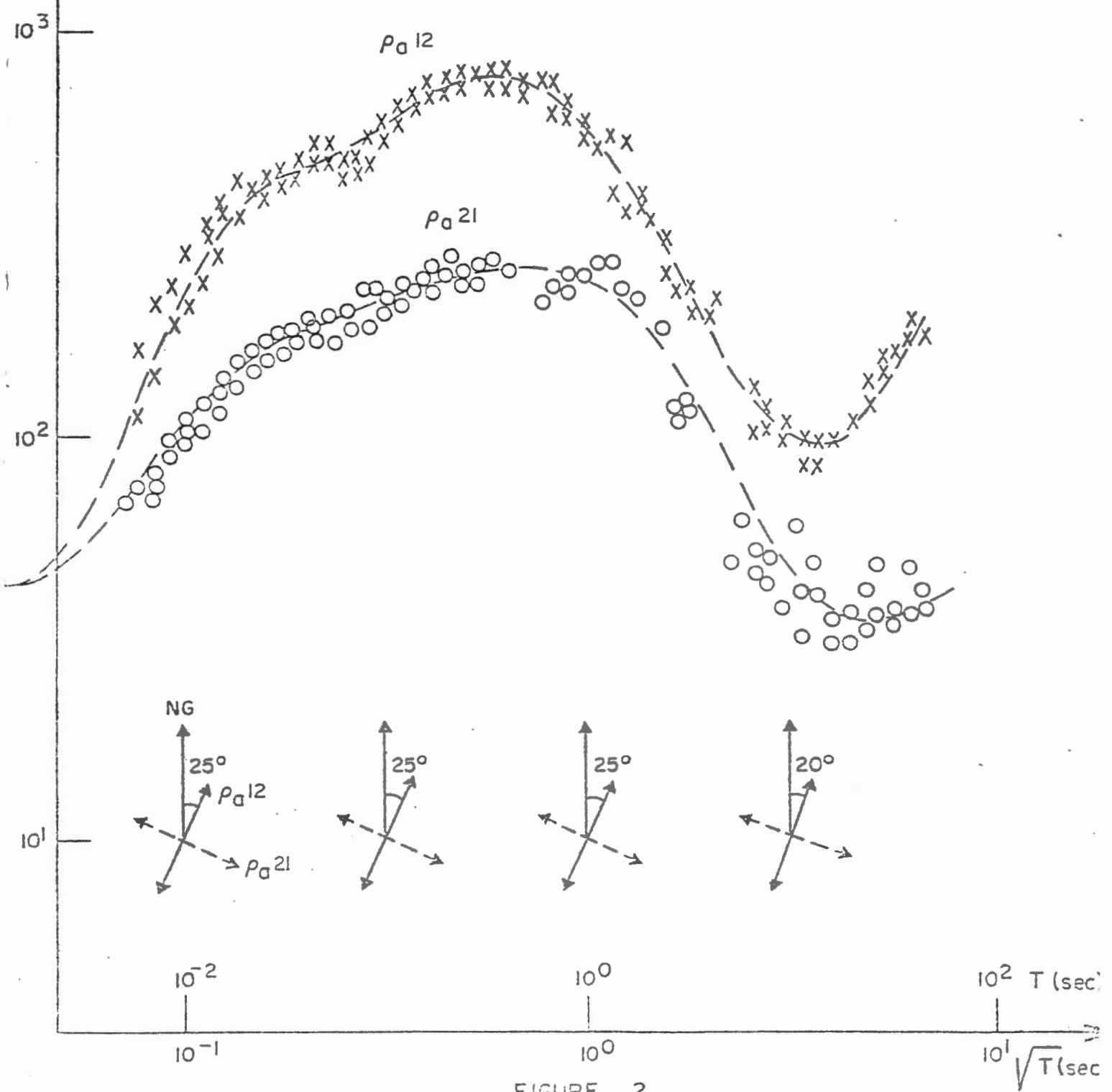


FIGURE 2

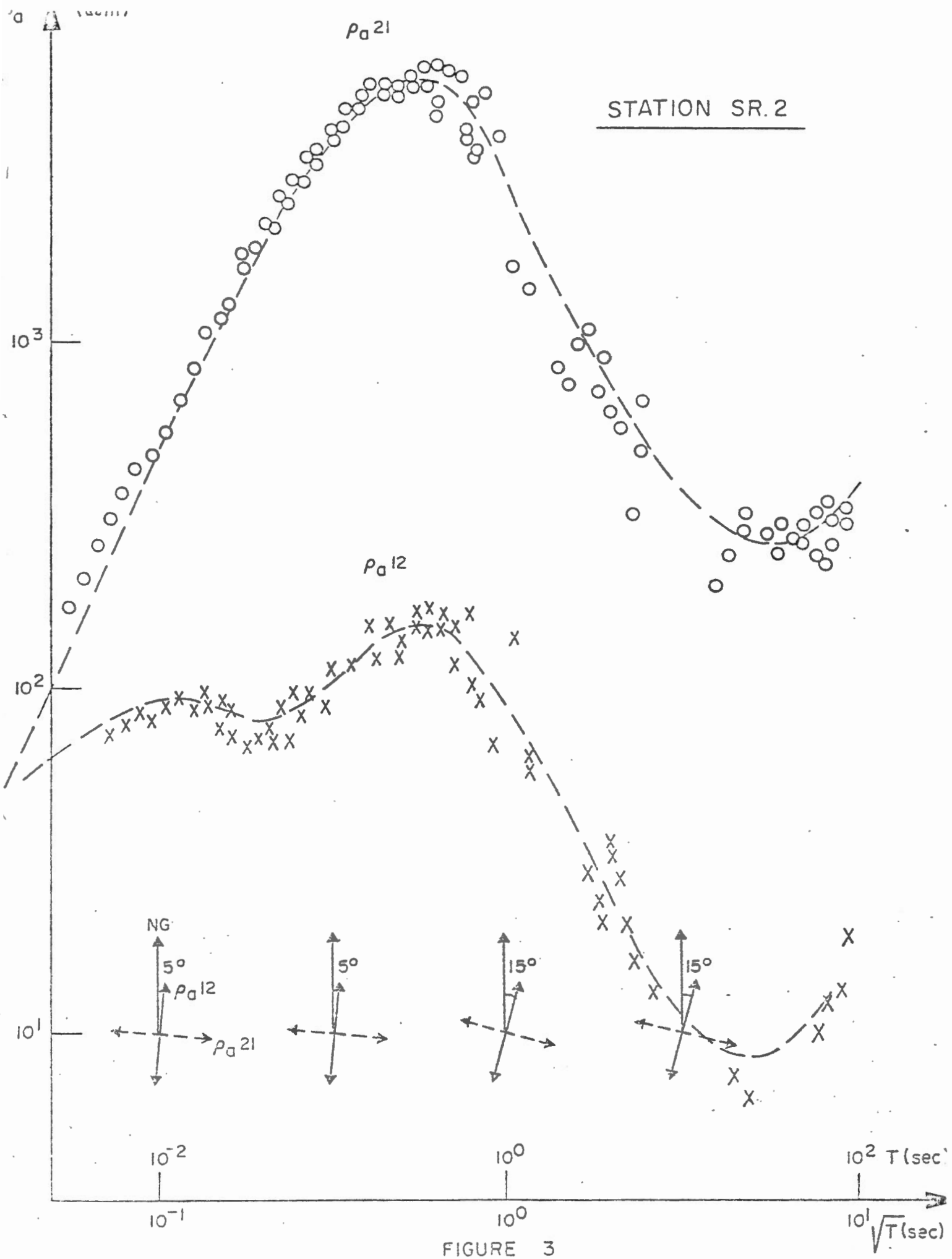


FIGURE 3

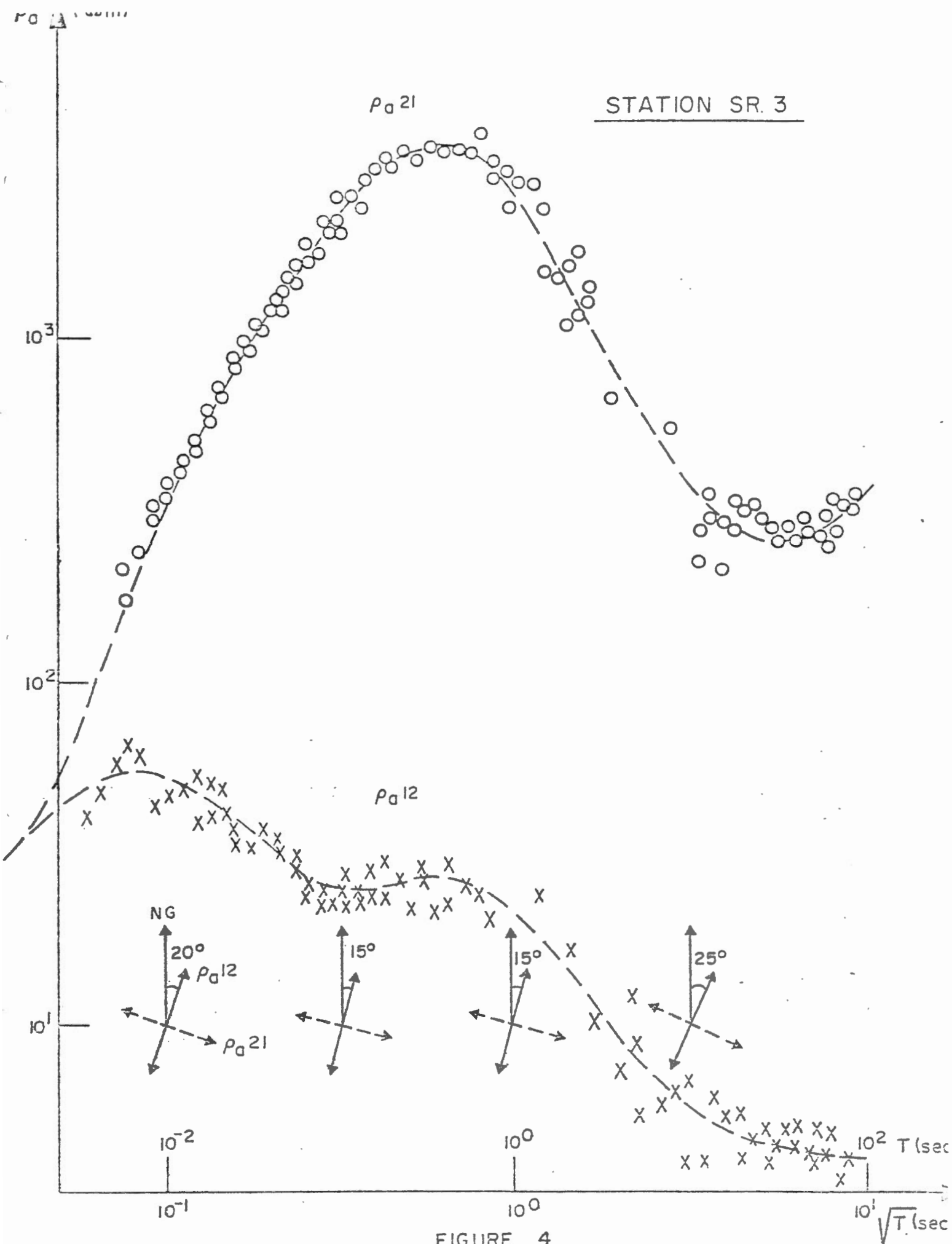


FIGURE 4

ρ_a

STATION SR. 4

$\rho_a 21$

$\rho_a 12$

10^3

10^2

10^1

10^{-2}

10^{-1}

10^0

10^0

$10^2 T(\text{sec})$

$10^1 \sqrt{T}(\text{sec})$

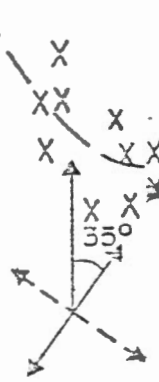
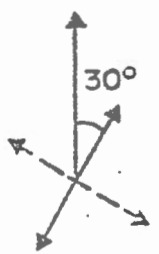
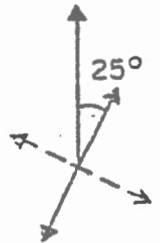
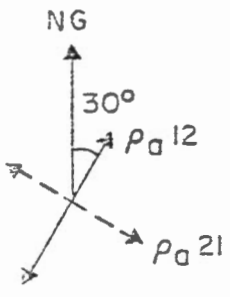


FIGURE 5

ρ_a (Ωm)

STATION SR.5

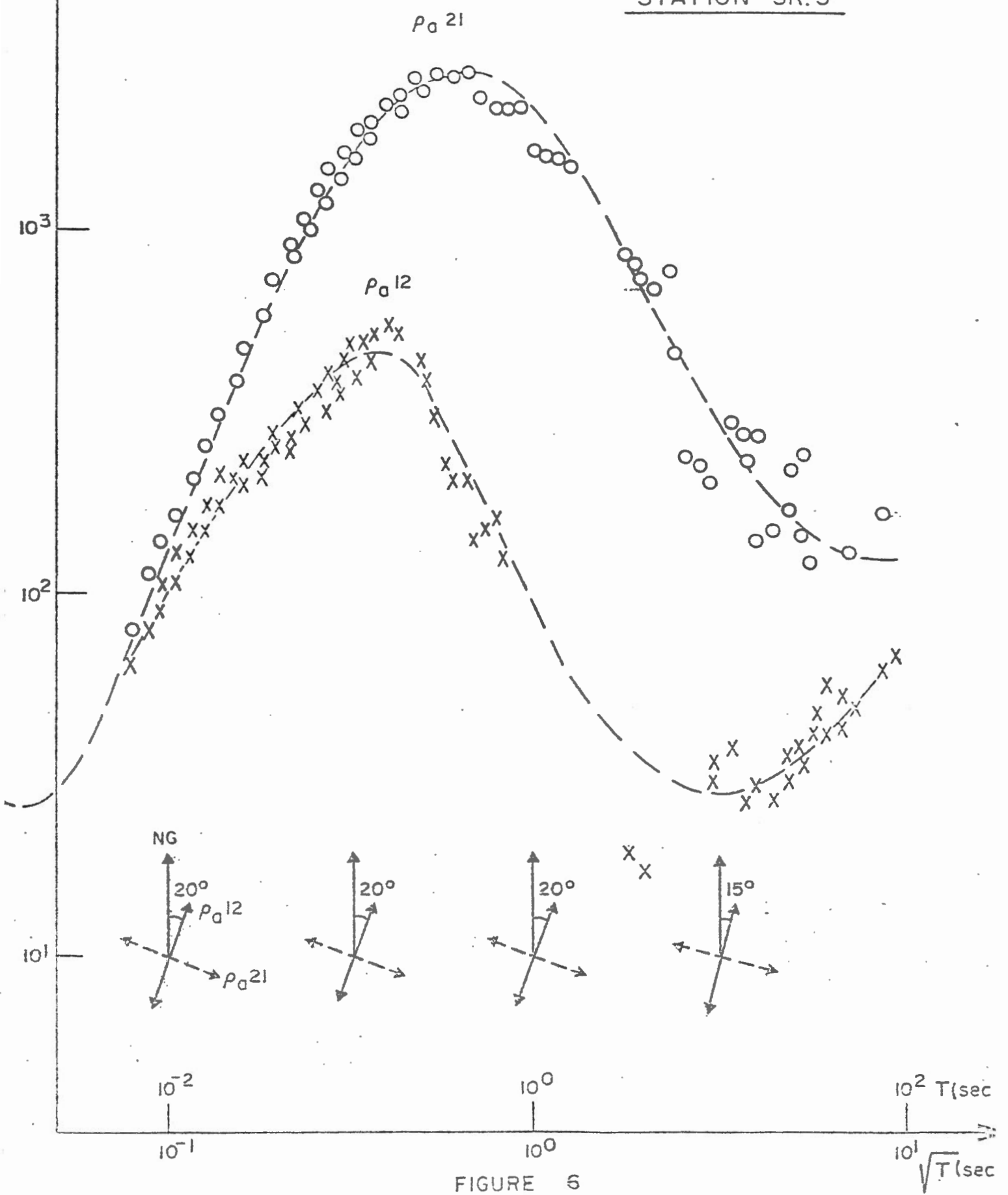


FIGURE 6

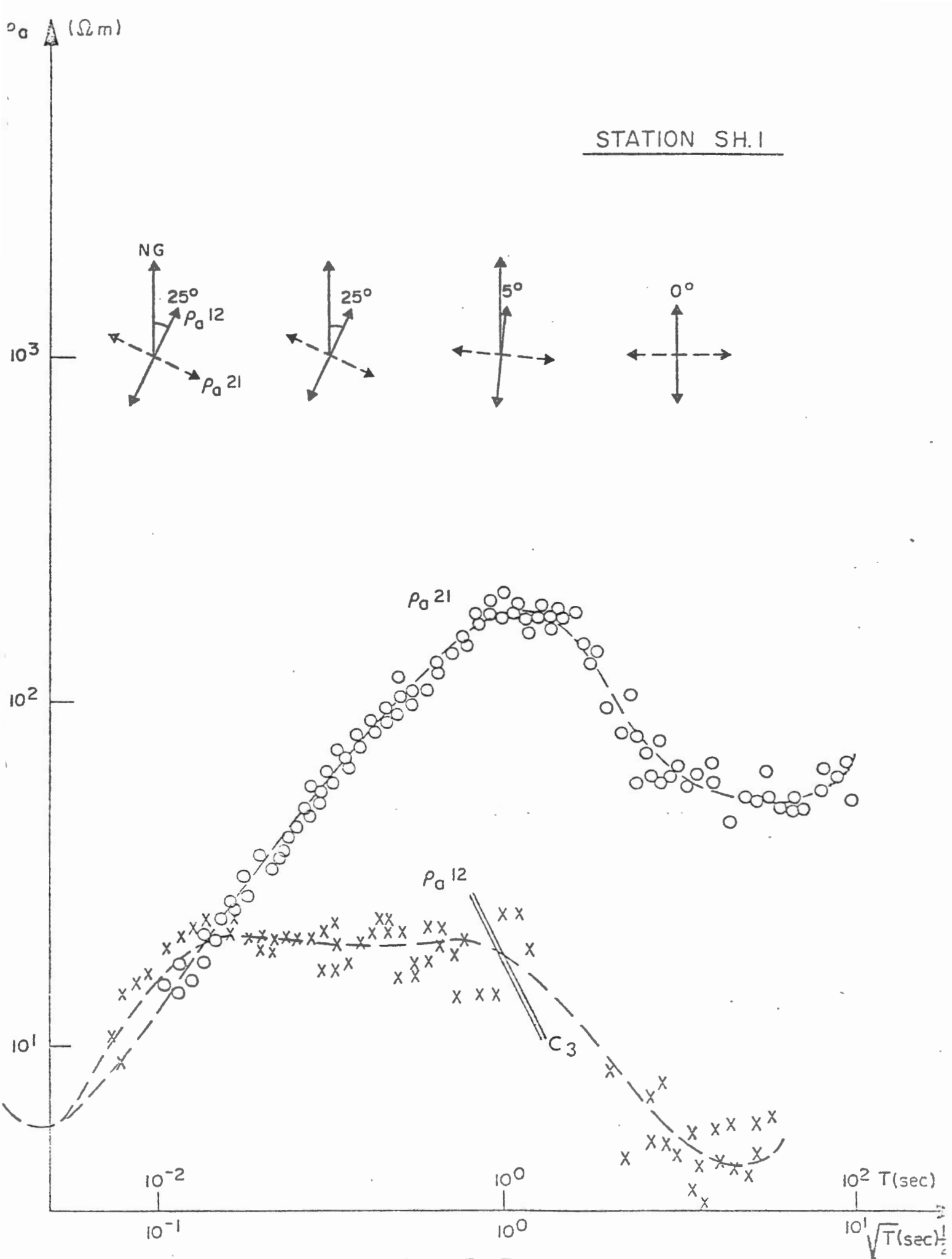


FIGURE 7

ρ_a (Ωm)

STATION SH. 2

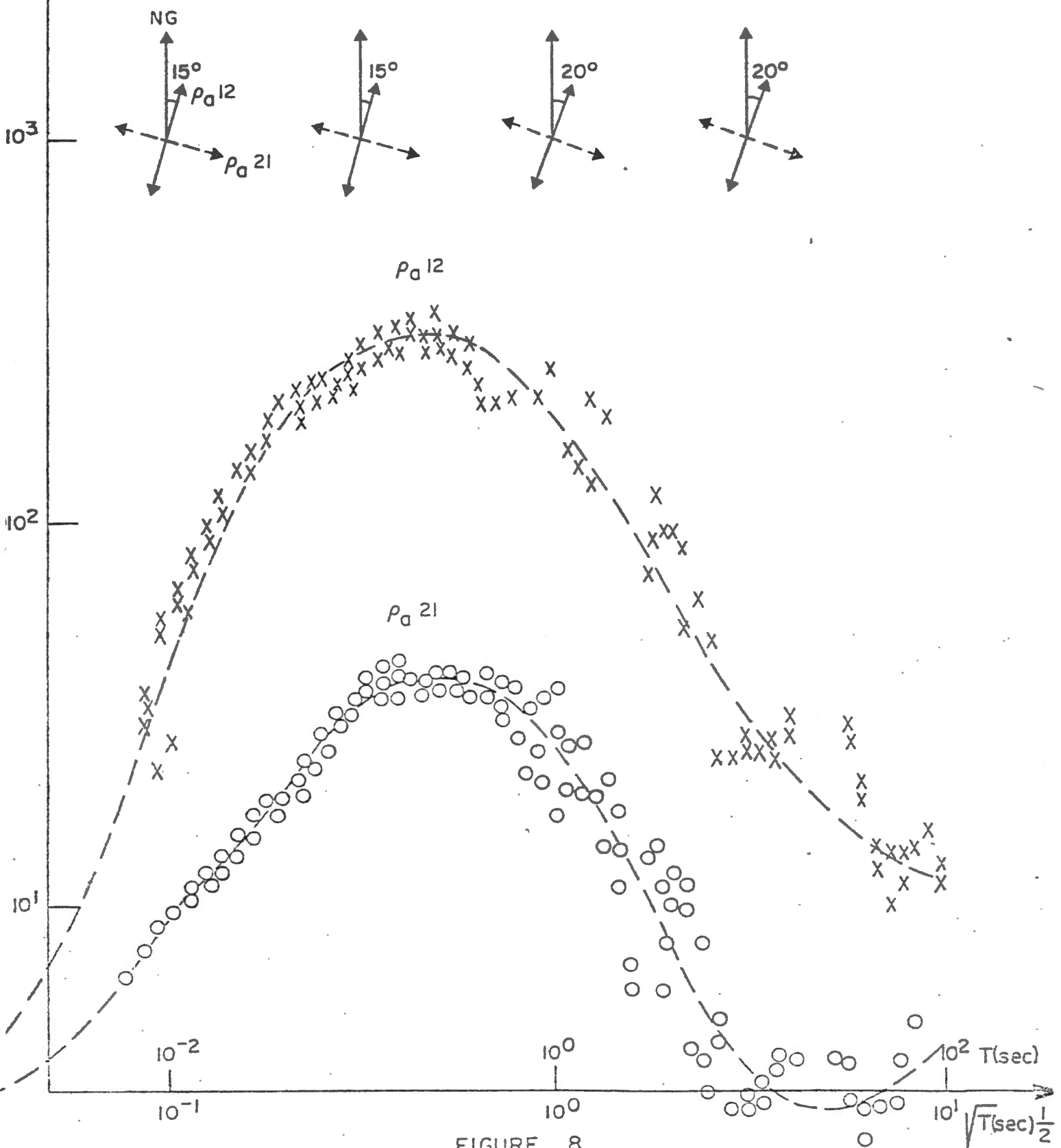


FIGURE 8

STATION SH. 3

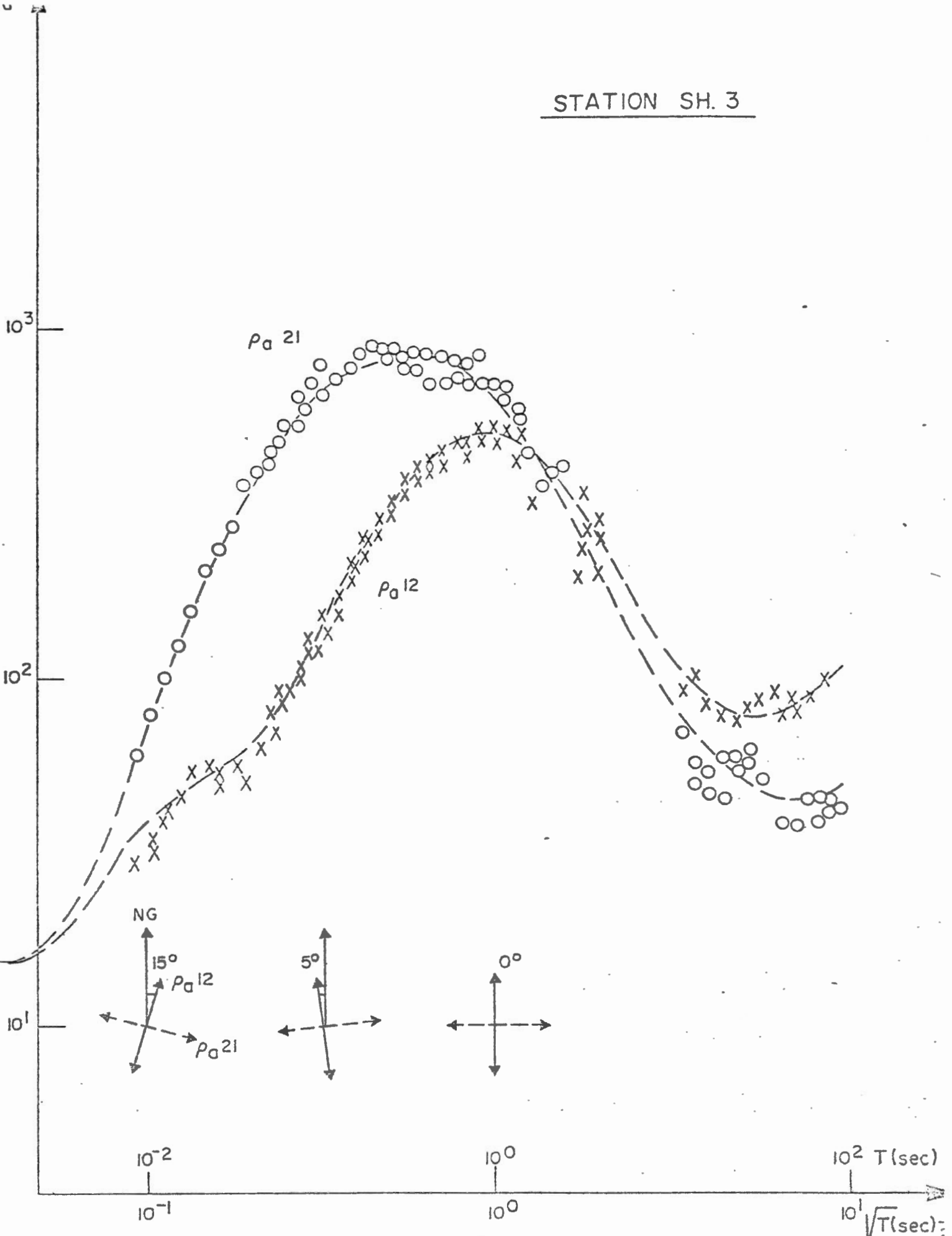


FIGURE 9

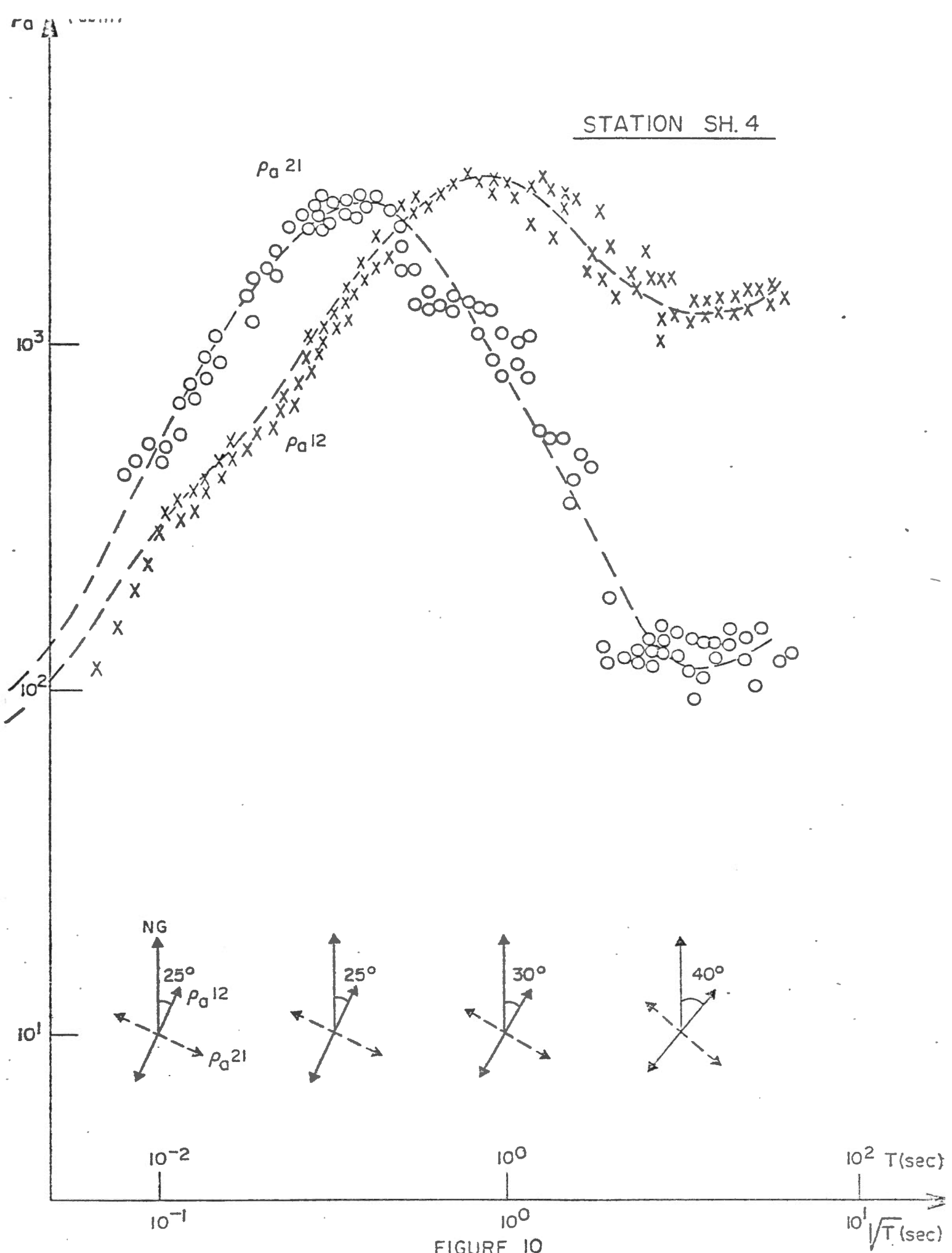


FIGURE 10

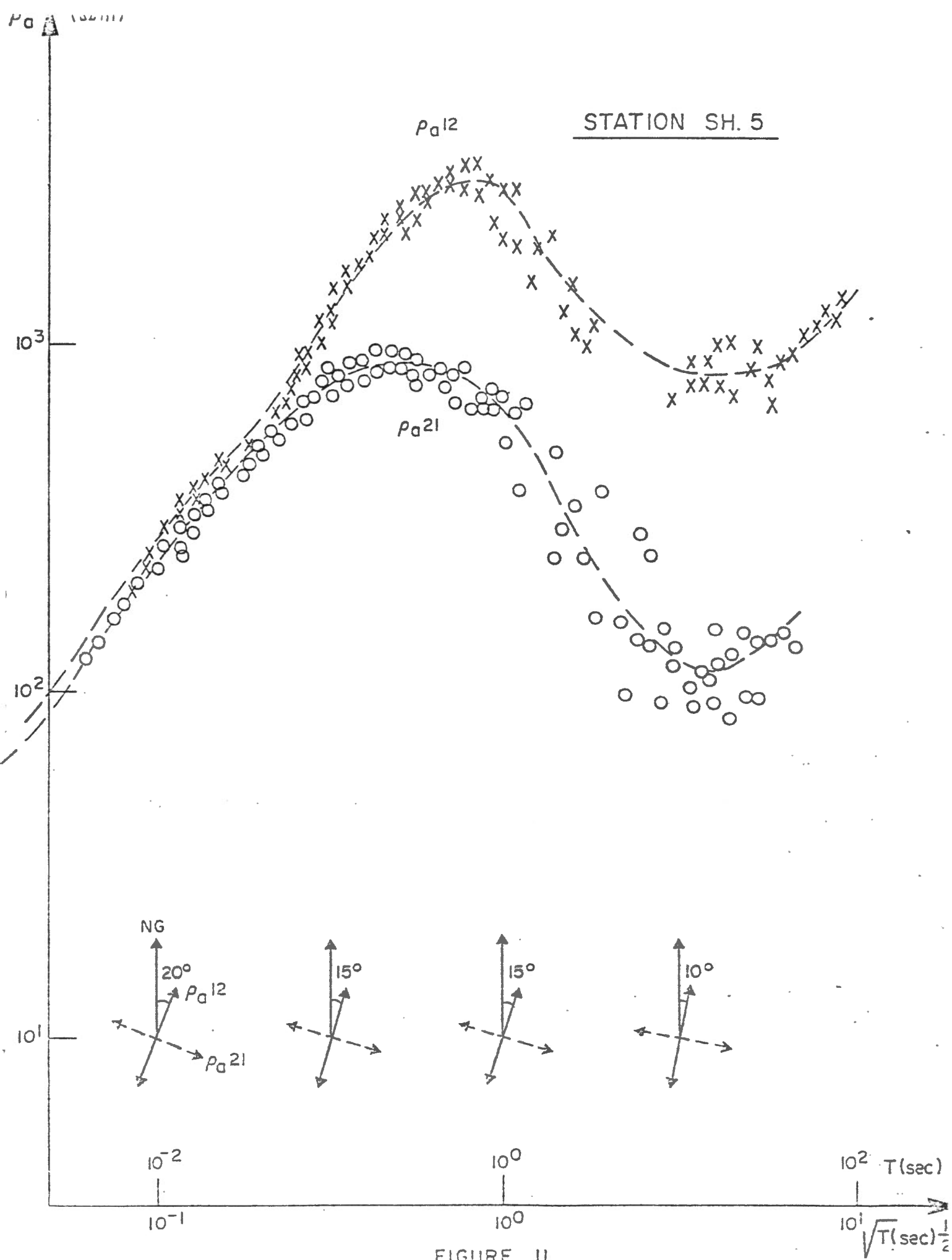
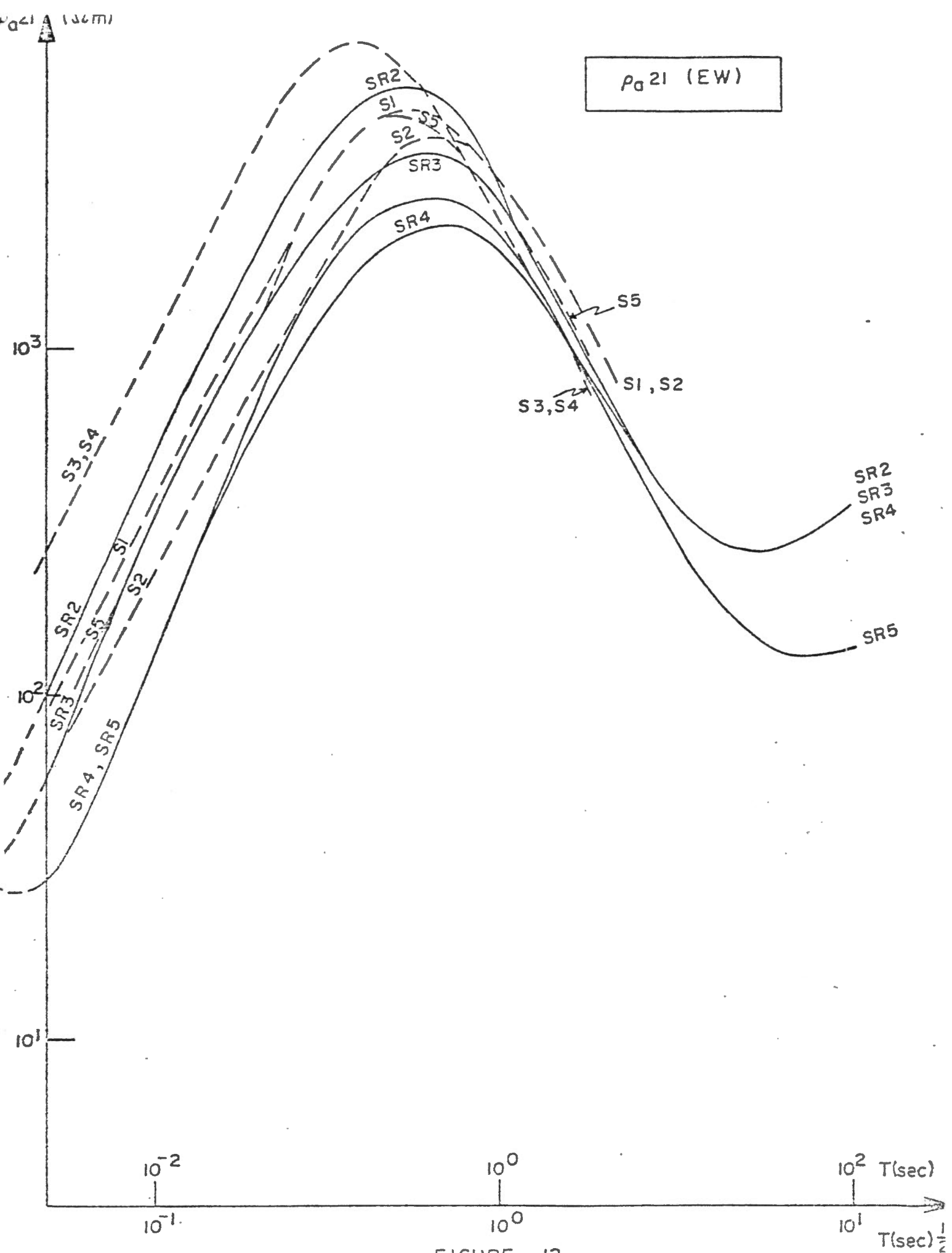


FIGURE II



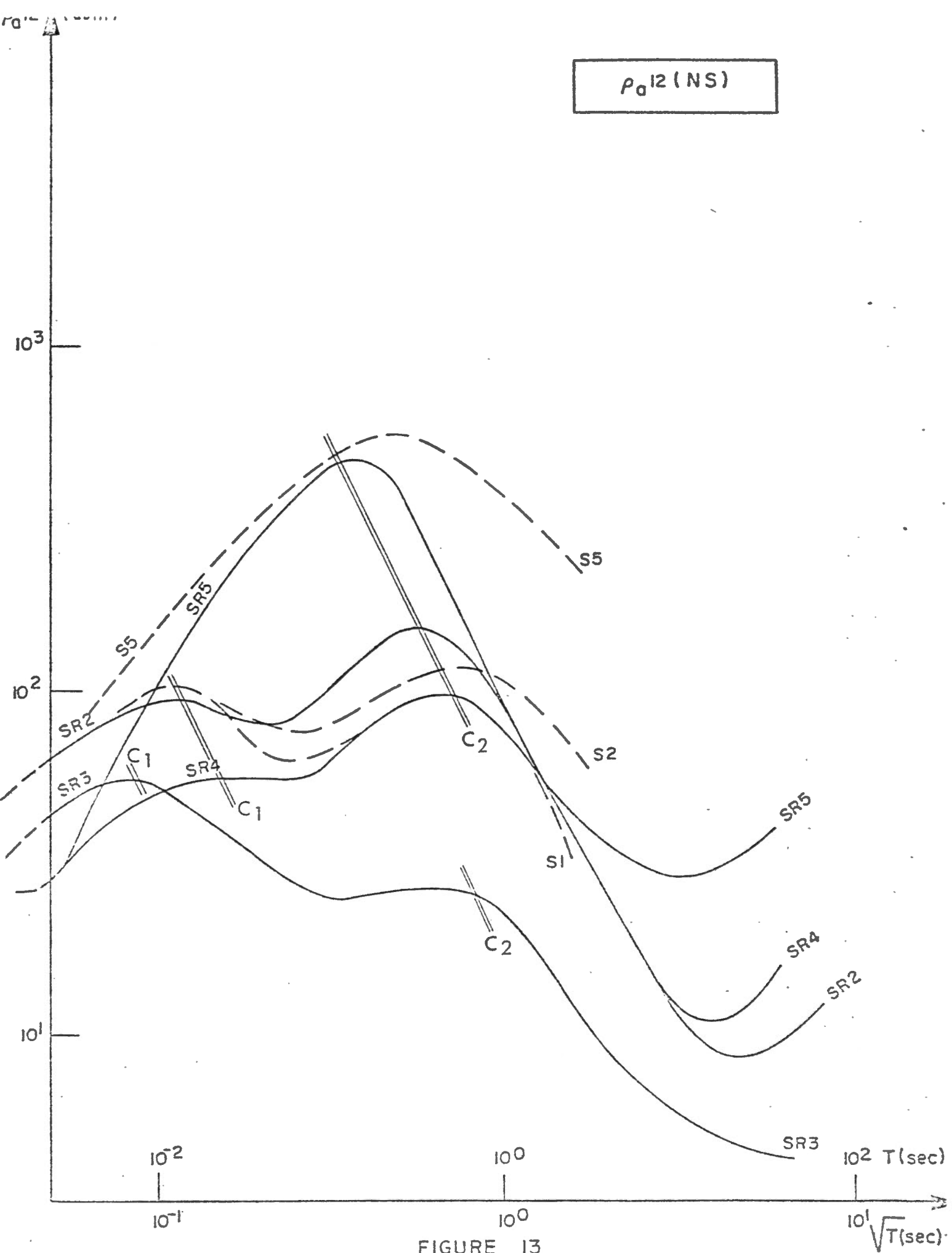


FIGURE 13

F = 100 Hz

562

561

560

559

5580000 mN

450000 mE

46

47

48

49

50

51



MI MEAGER 

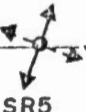
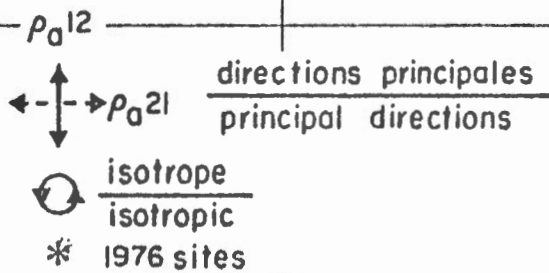


FIGURE 14



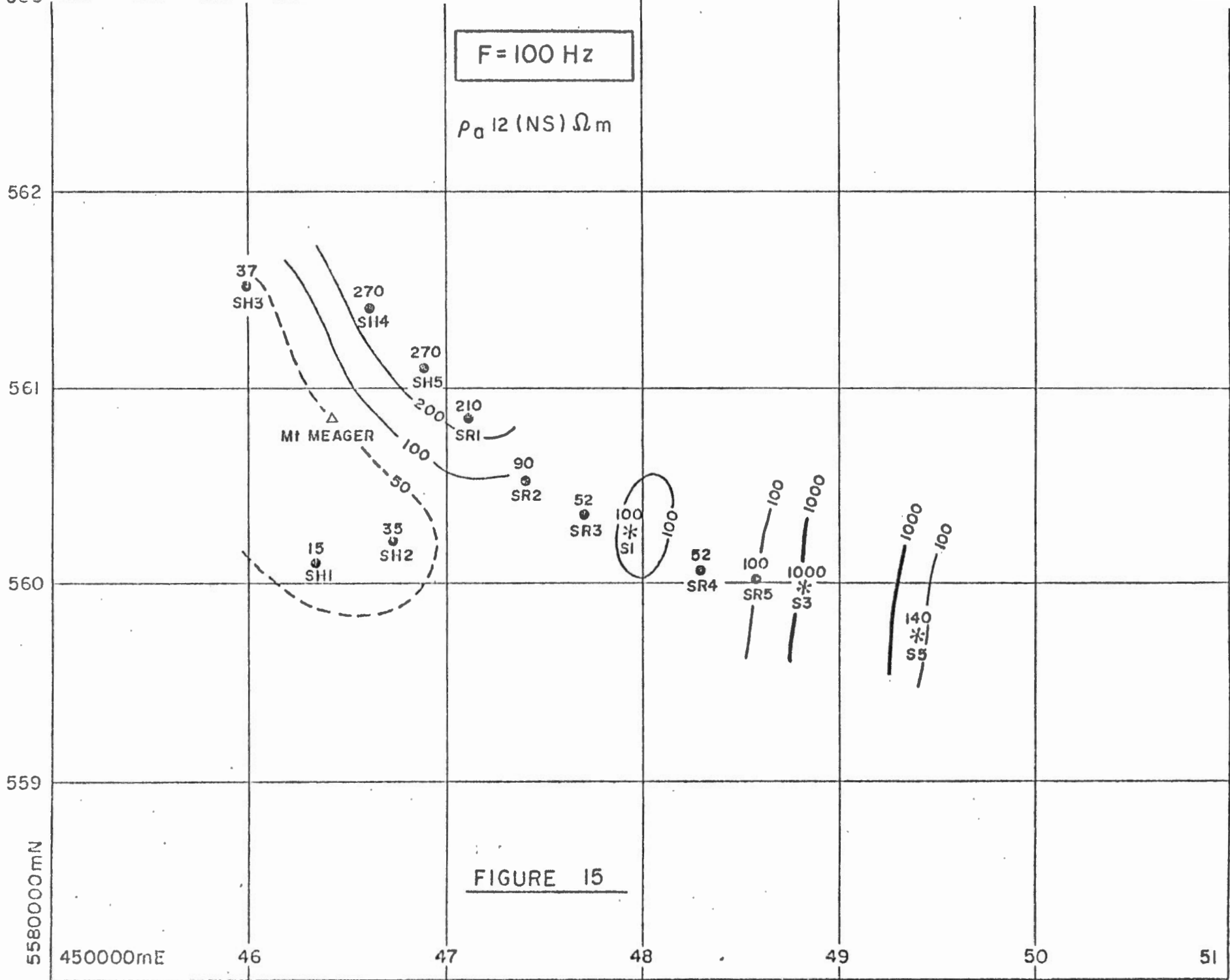


FIGURE 15

F = 100 Hz

$\rho_a 2l (EW) \Omega m$

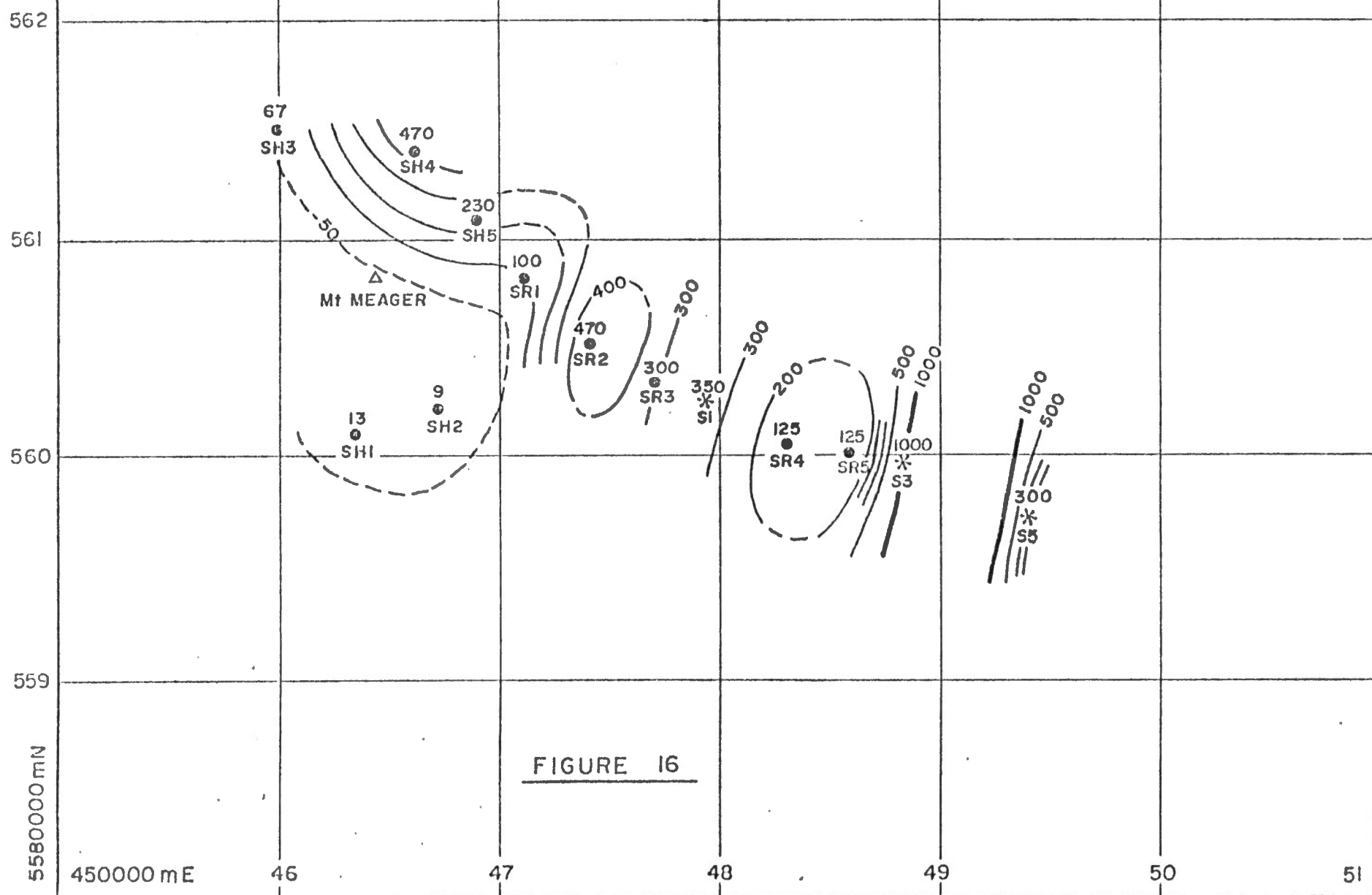


FIGURE 16

F = 1 Hz

562

561

560

559

5580000mN

450000mE

46

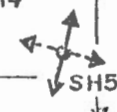
47

48

49

50

51



MI MEAGER

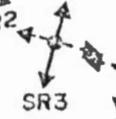




FIGURE 17

$\rho_a 12$
 $\rho_a 21$ directions principales
principal directions
 isotrope
isotropic.
* 1976 sites

F = 1 Hz

ρ_{012} (NS)

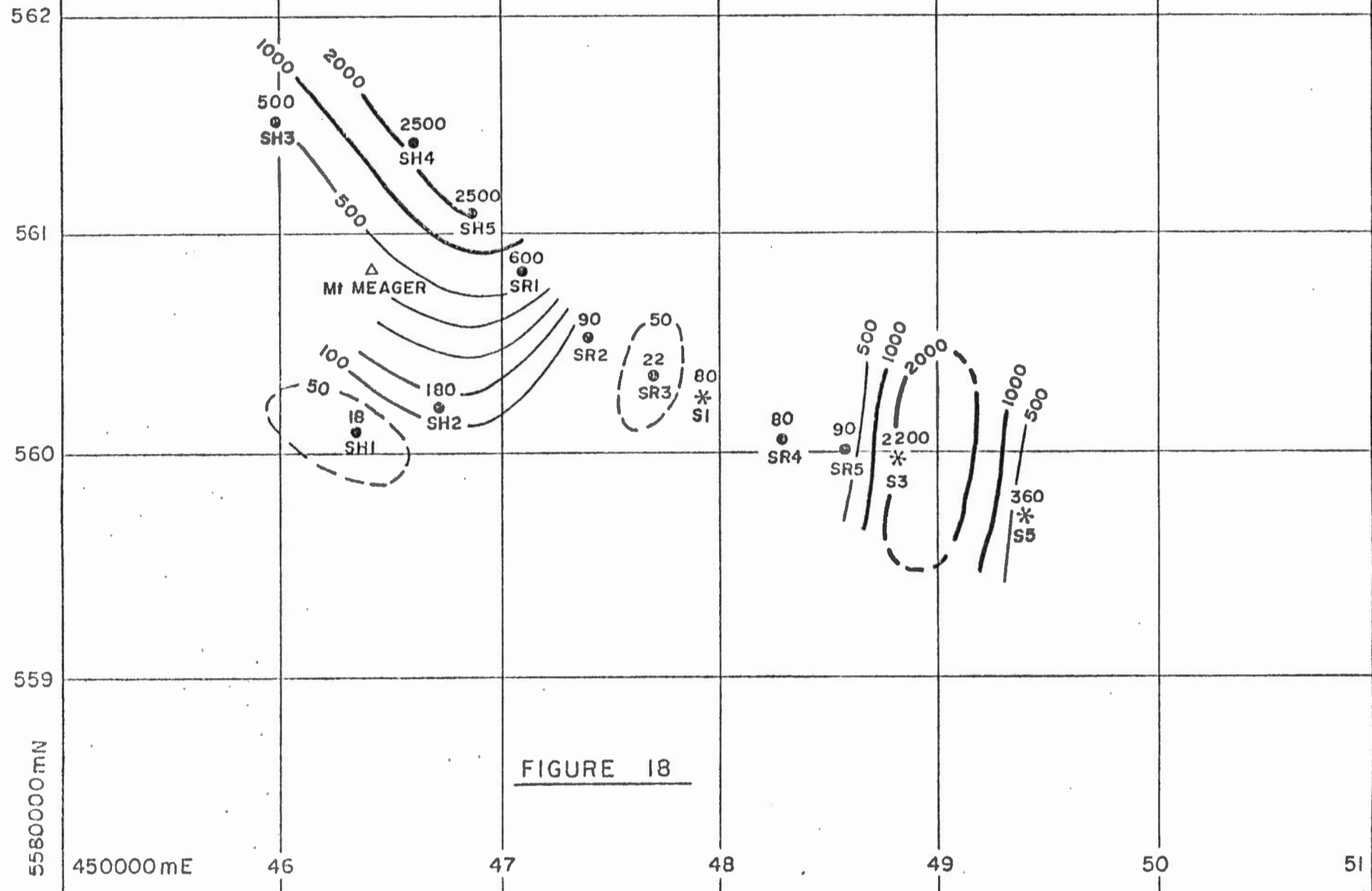
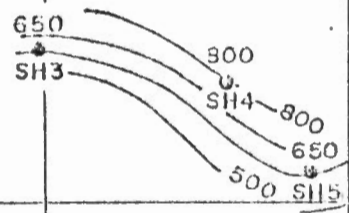


FIGURE 18

F = 1 Hz

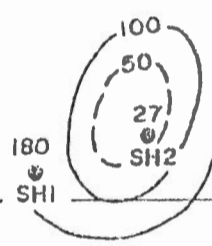
$\rho_a 21 (EW) \Omega m$

562

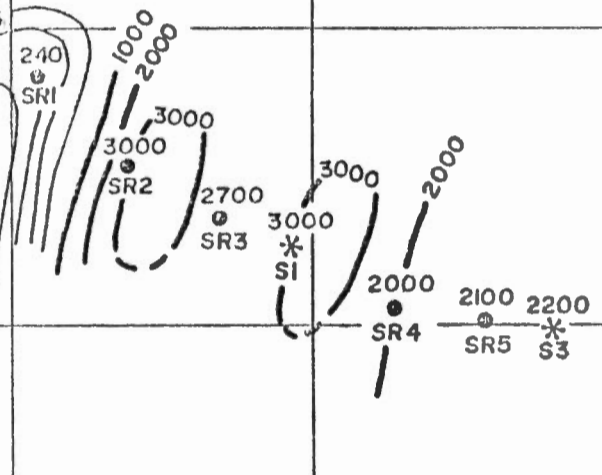


561

MI MEAGER



560



559

FIGURE 19

5580000 mN

450000 mE

46

47

48

49

50

51

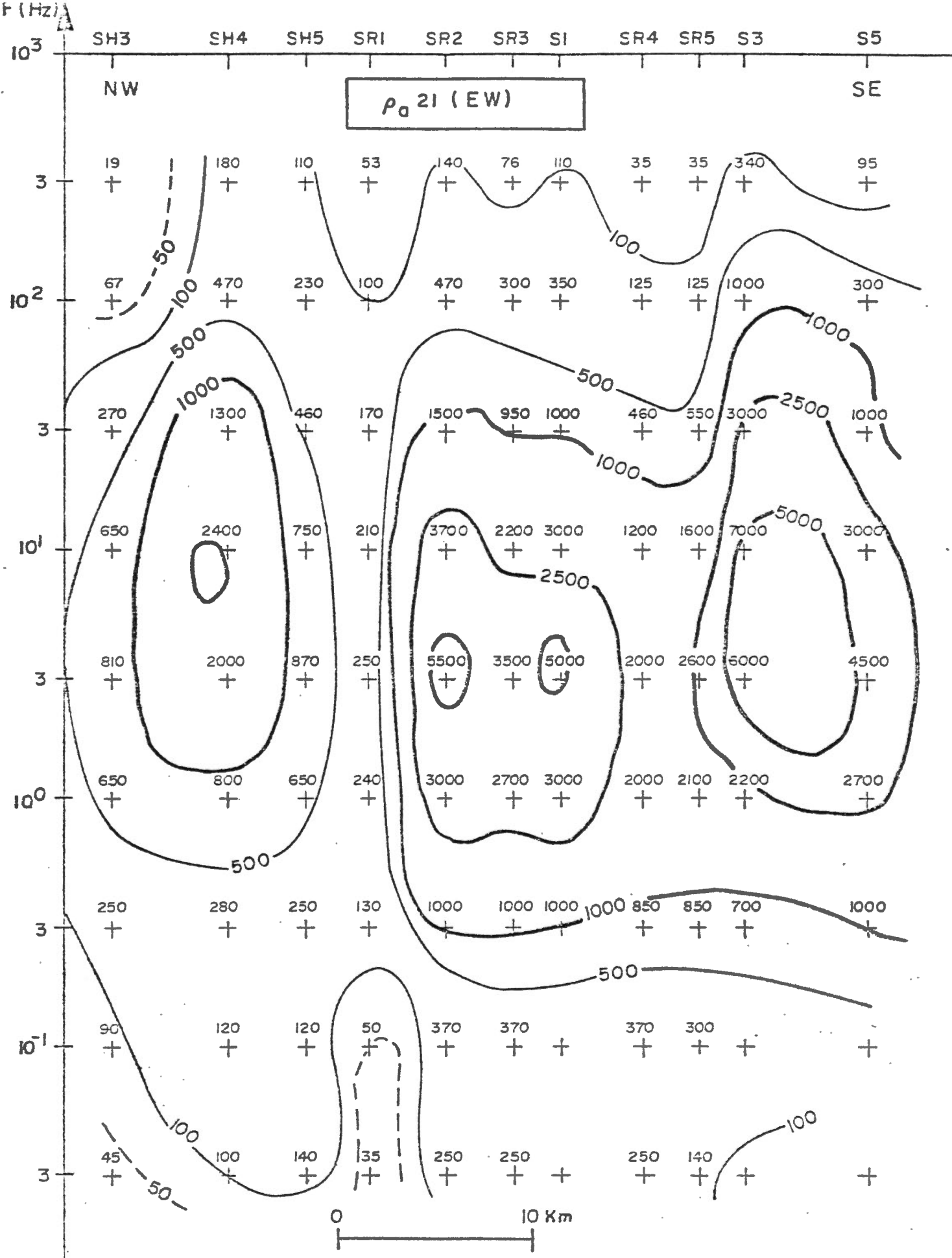


FIGURE 20: PSEUDO-SECTION PROFIL
PROFILE A

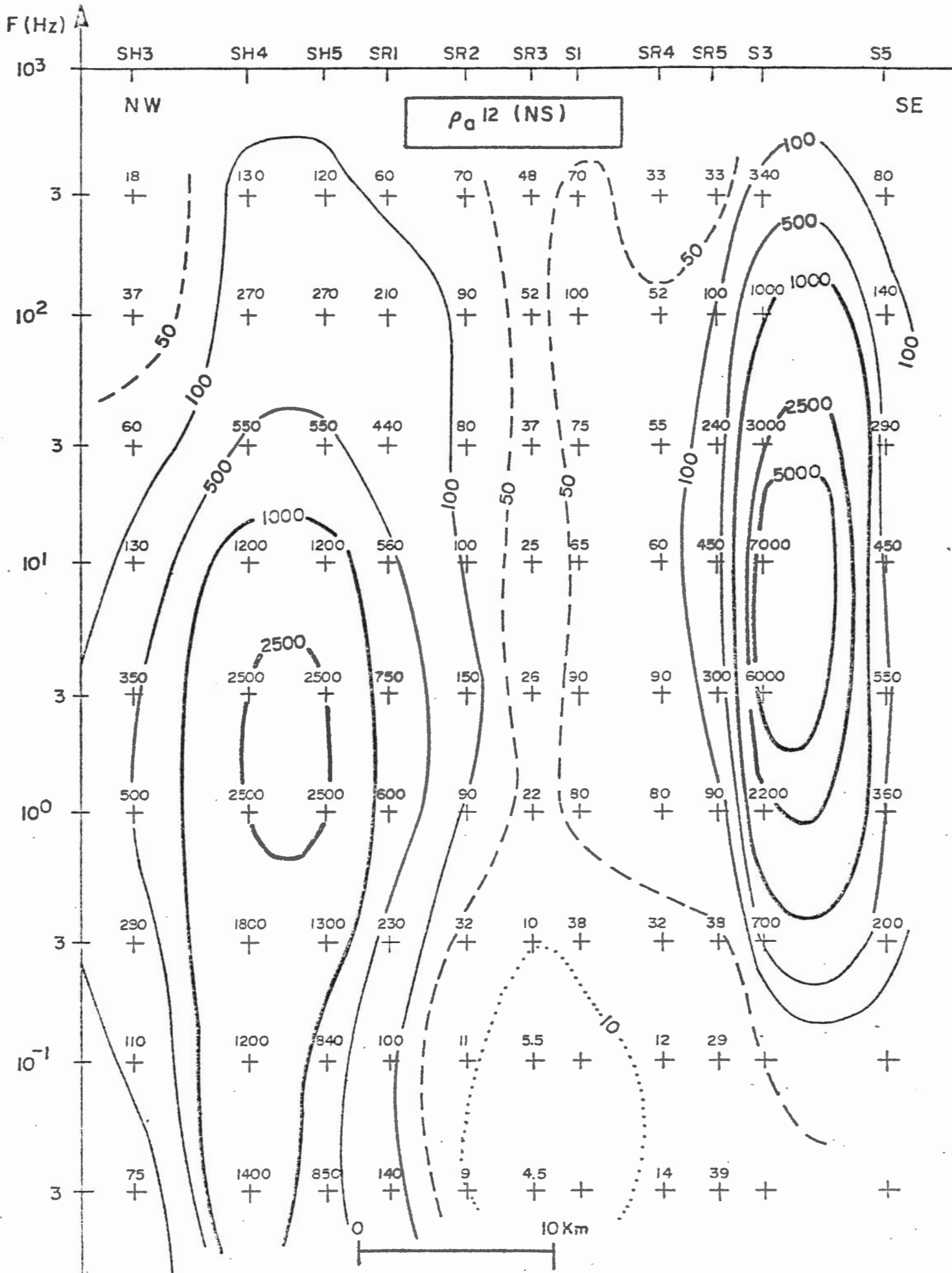
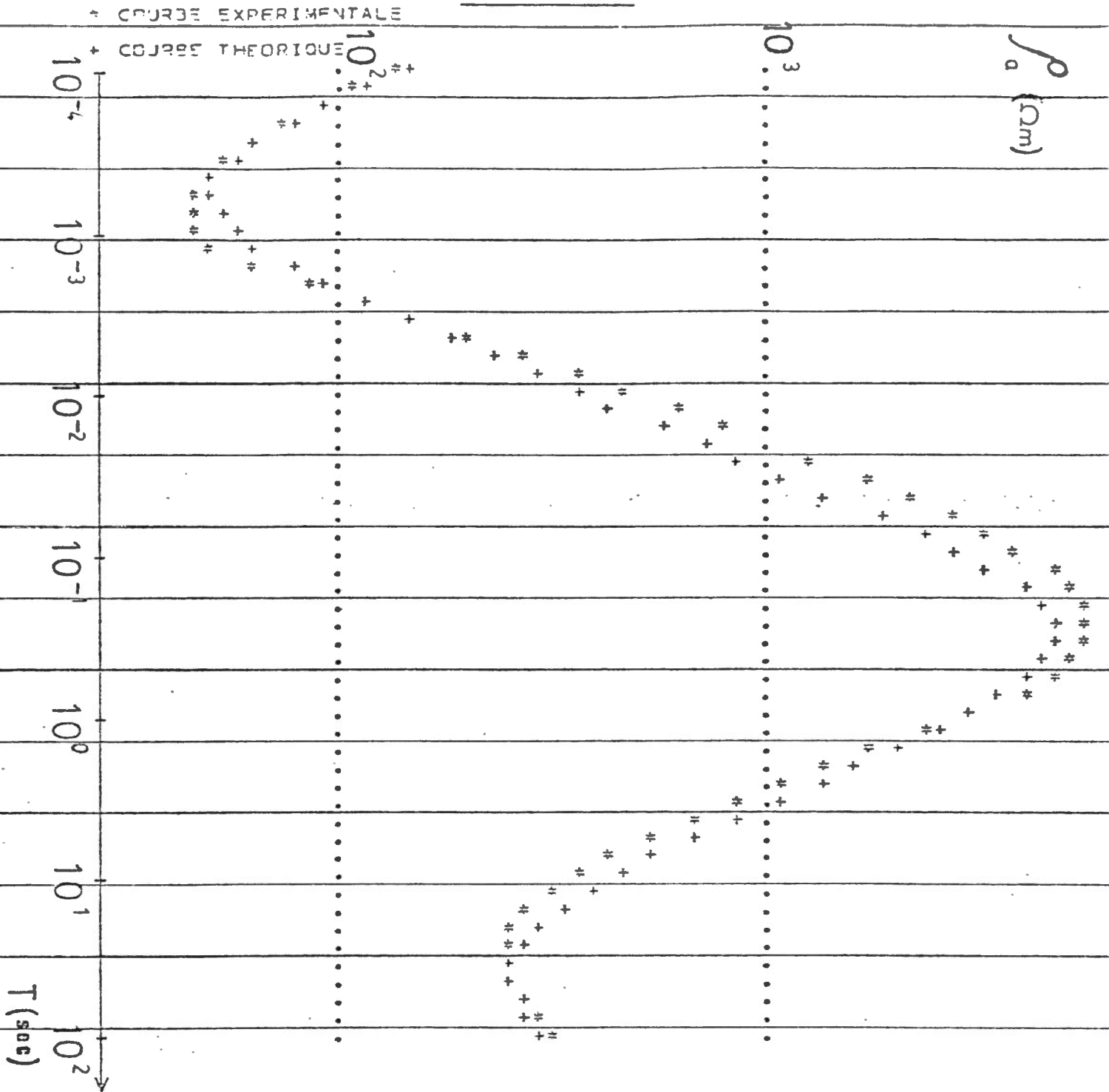


FIGURE 21 : PSEUDO-SECTION $\rho_a 12$ (NS) PROFILE A



STATION SR.2

PO 1 = 0.100000E 04 Ω m H 1 = 0.430000E -01 km

PO 2 = 0.210000E 01 H 2 = 0.350000E -02

PO 3 = 0.200000E 05 H 3 = 0.190000E 02

PO 4 = 0.600000E 02 H 4 = 0.100000E 02

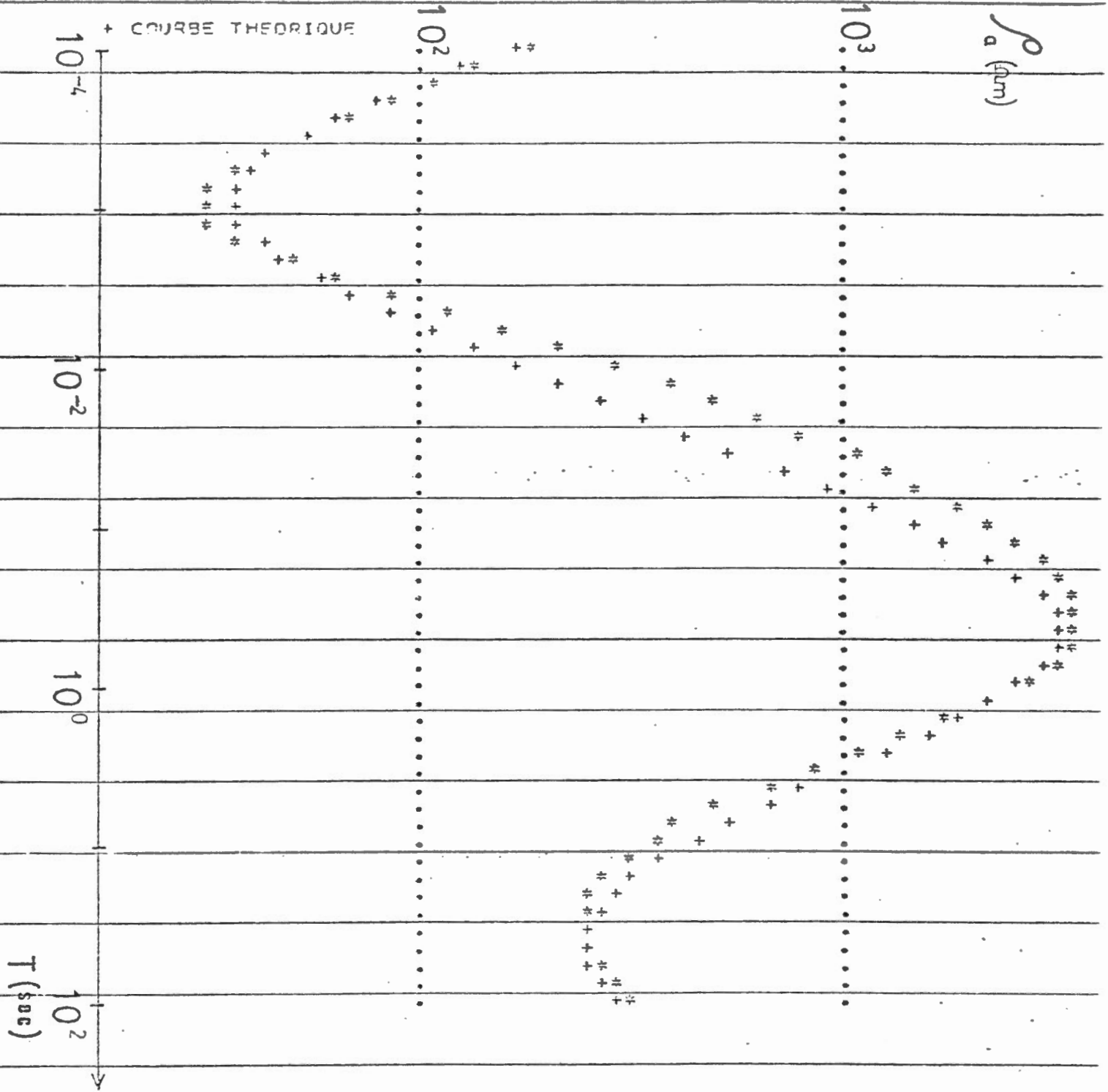
PO 5 = 0.100000E 04 H 5 = ∞

STATION SR.3

FIGURE 23

COURSE EXPERIMENTALE

+ COURSE THEORIQUE



STATION SR.3

RC 1 = 0.100000E 04 Ω m H 1 = 0.450000E-01 km

RC 2 = 0.200000E 01 H 2 = 0.500000E-02

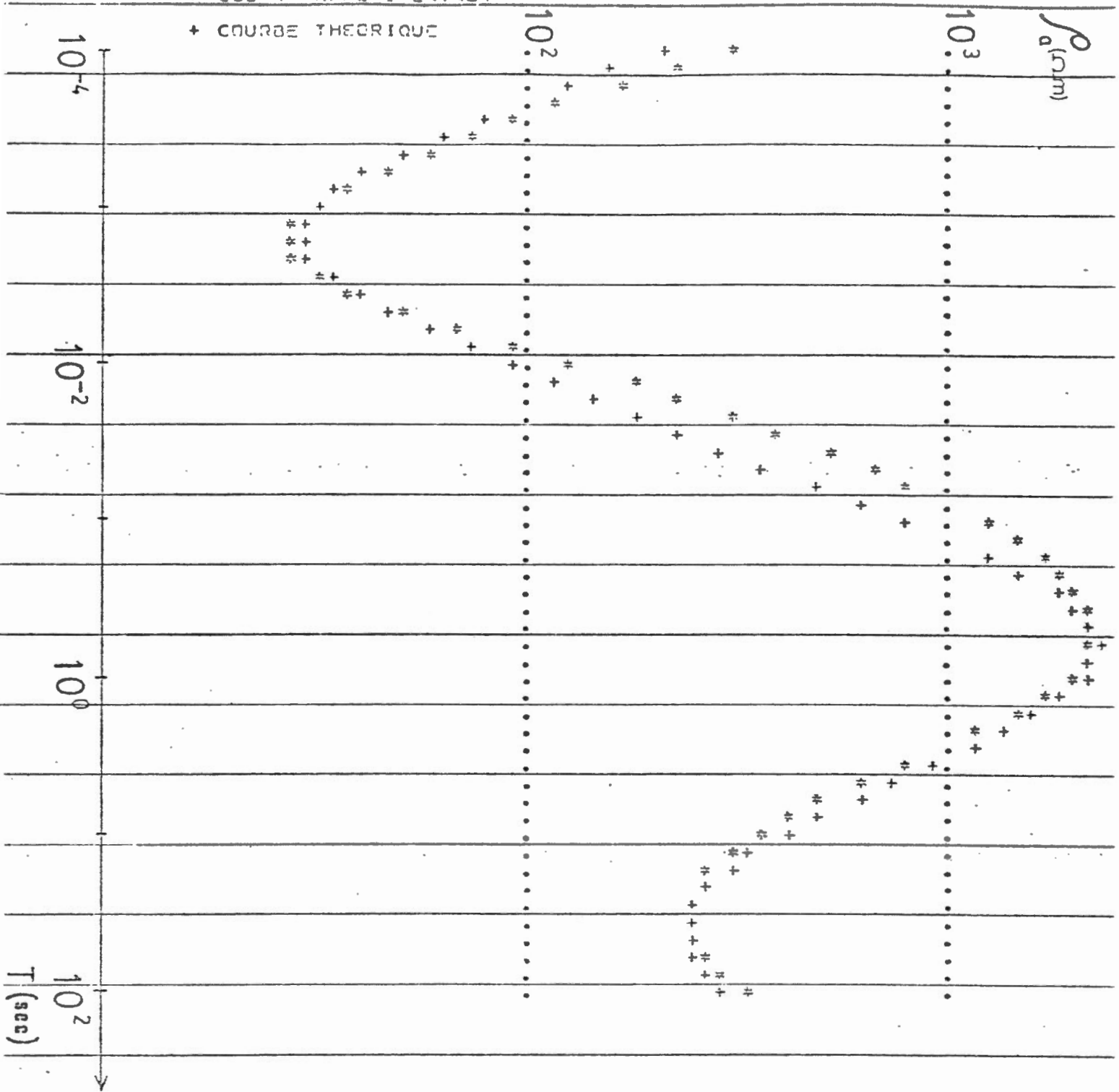
RC 3 = 0.200000E 05 H 3 = 0.100000E 02

RC 4 = 0.600000E 02 H 4 = 0.100000E 02

RC 5 = 0.100000E 04 H 5 = 8

* COURSE EXPERIMENTALE

+ COURSE THEORIQUE



STATION SR.4

01 1 = 0.300000E 04 Ω m H 1 = 0.500000E-01 km

01 2 = 0.110000E 01 H 2 = 0.400000E-02

01 3 = 0.200000E 05 H 3 = 0.180000E 02

01 4 = 0.600000E 02 H 4 = 0.100000E 02

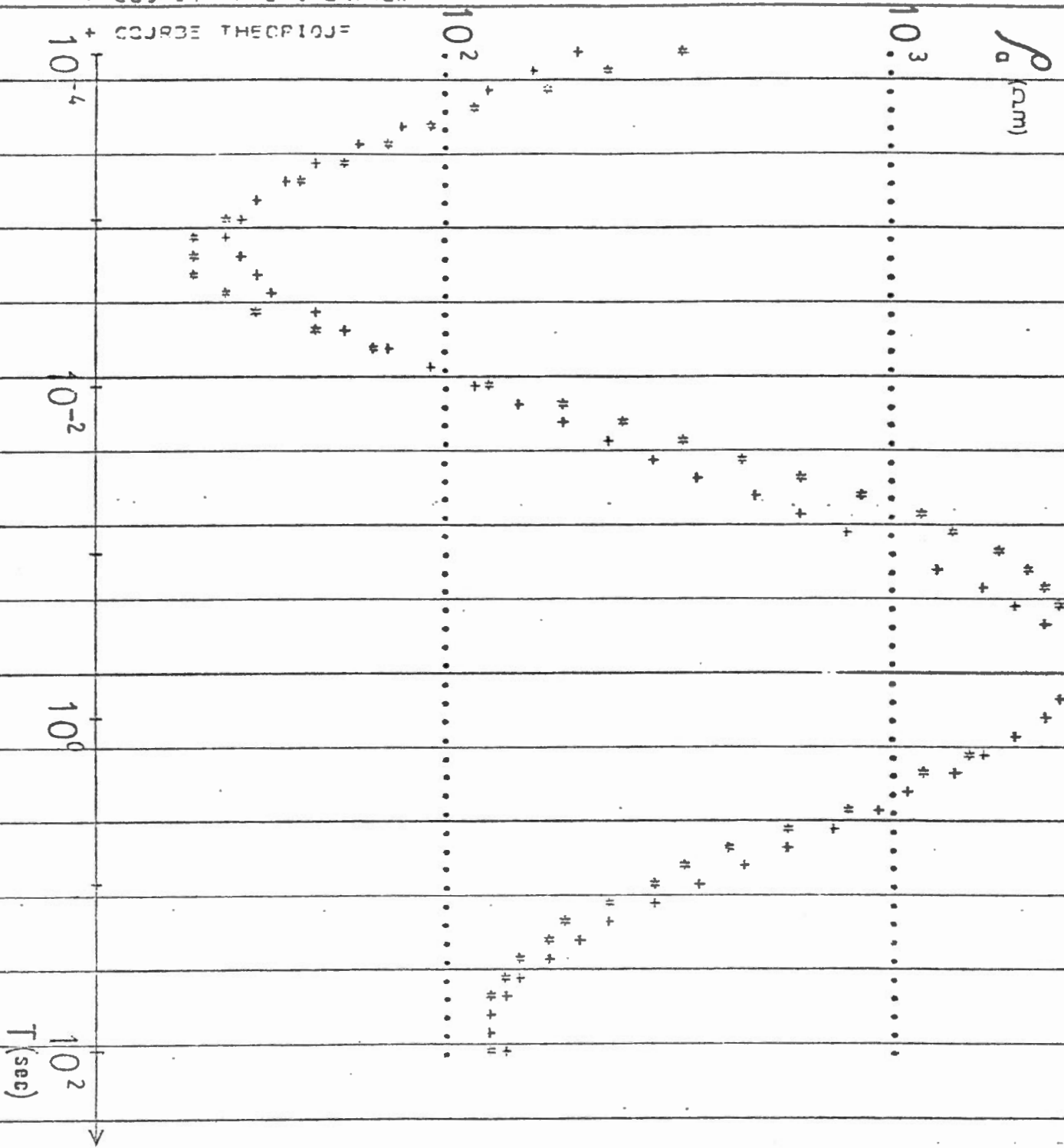
01 5 = 0.100000E 04 H 5 = ∞

STATION BR.5

FIGURE 25

* COURSE EXPERIMENTALE

+ COURSE THEORIQUE



STATION BR.5

RC 1 = 0.300000E 04 Ω m H 1 = 0.500000E-01 km

RC 2 = 0.110000E 01 H 2 = 0.350000E-02

RC 3 = 0.250000E 05 H 3 = 0.120000E 02

RC 4 = 0.300000E 02 H 4 = 0.100000E 02

RC 5 = 0.100000E 04 H 5 = ∞

SONDAGE M. T.

STATION A

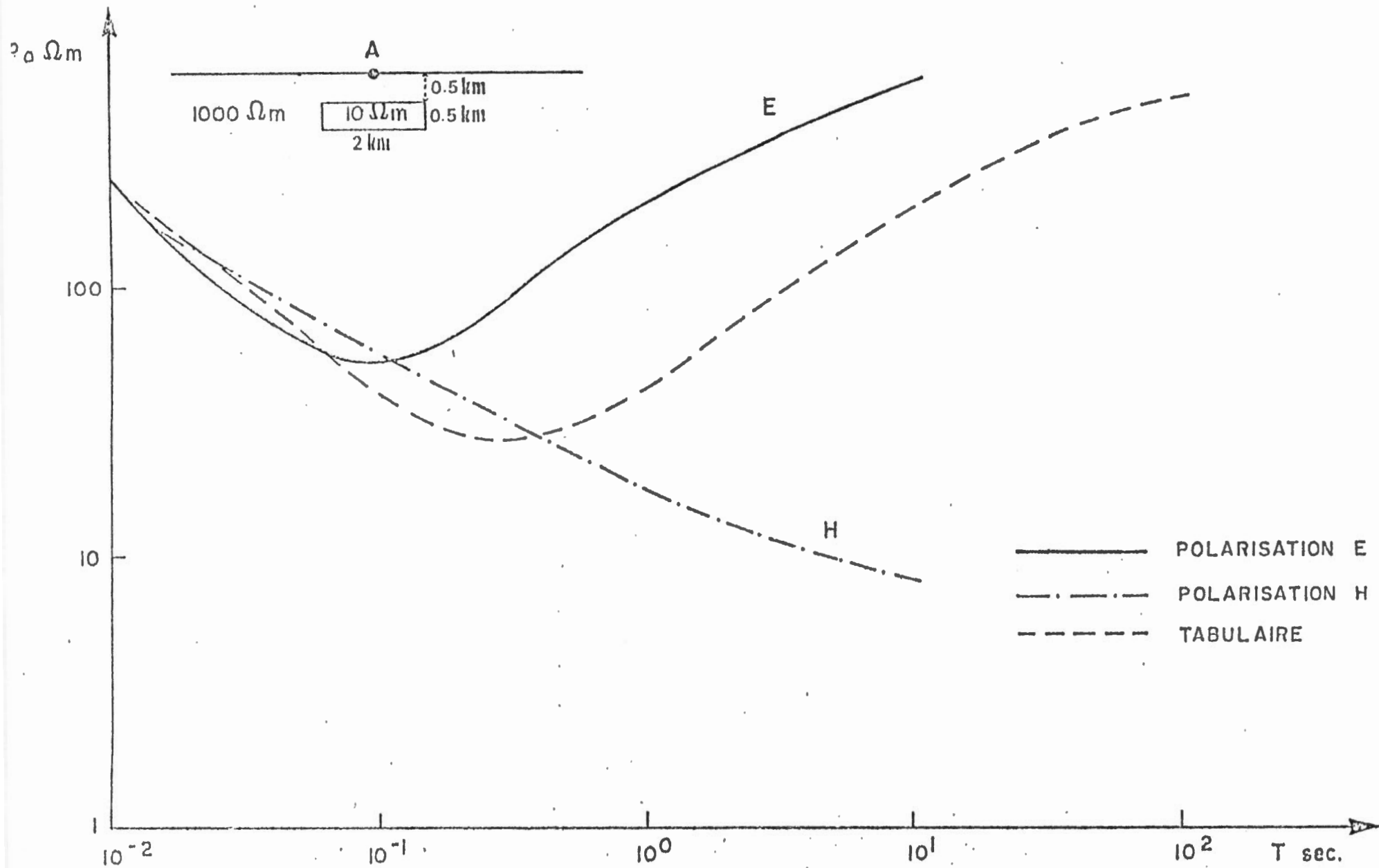


FIGURE 26.

SONDAGE M.T.

STATION C

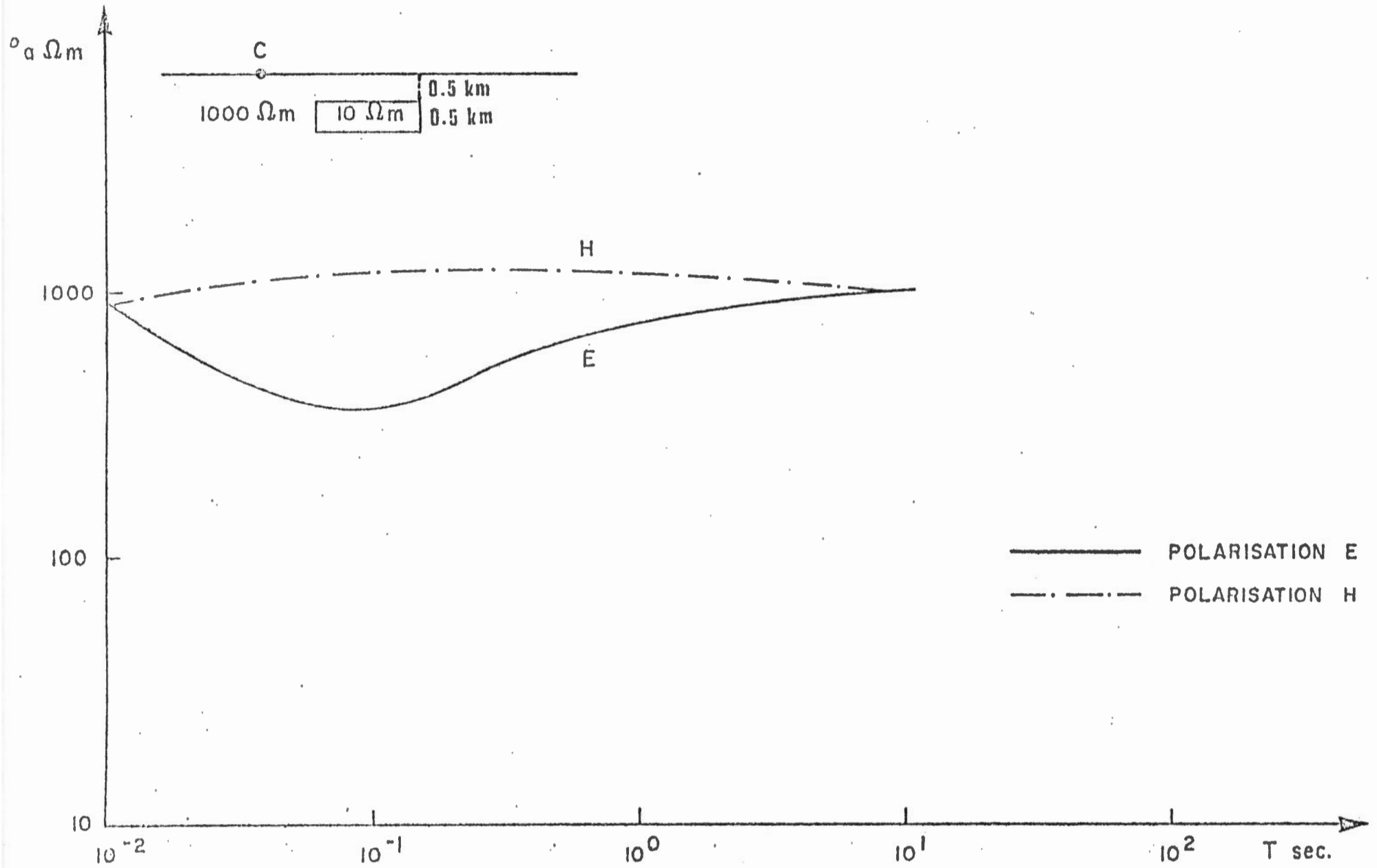
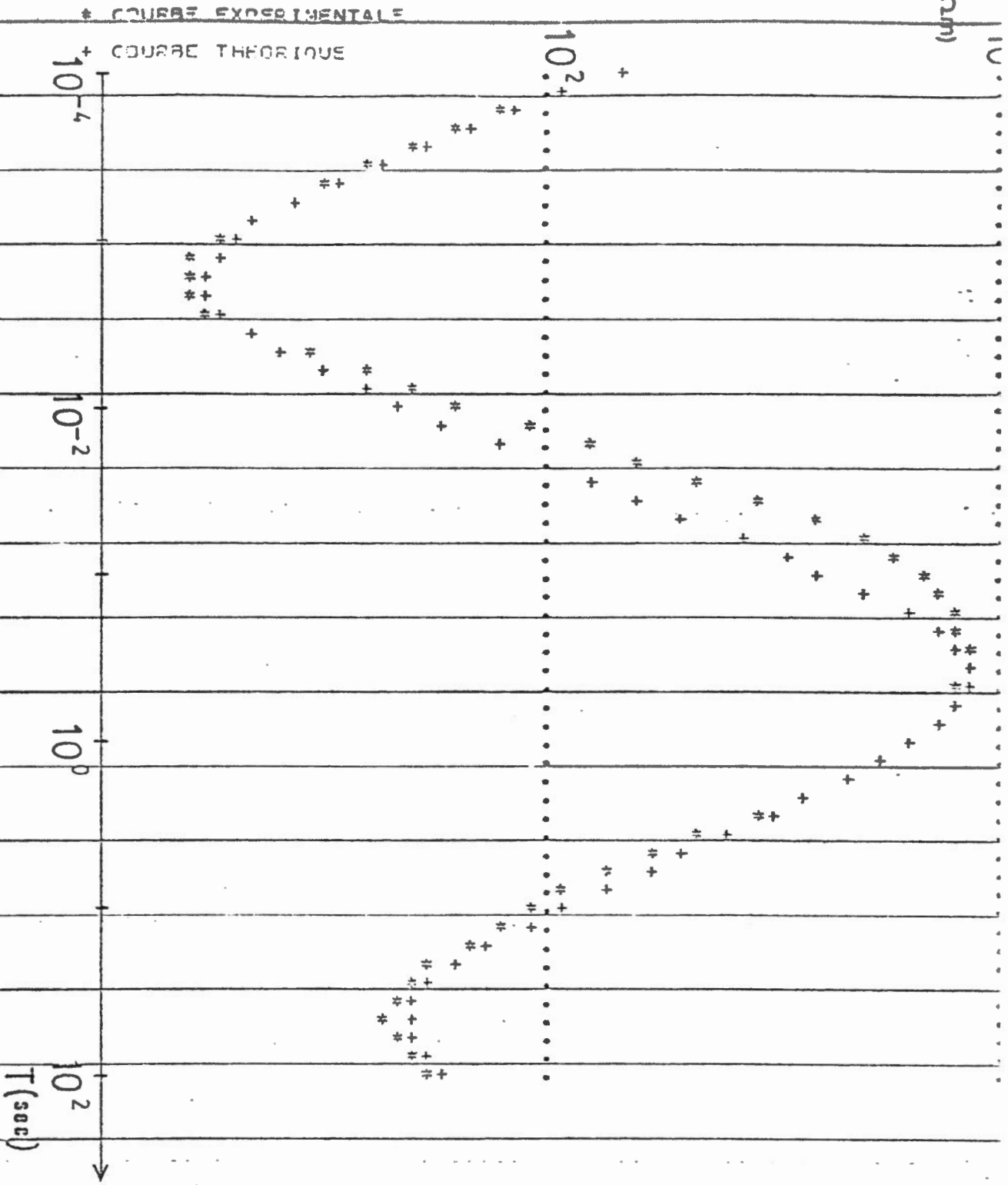


FIGURE 27

STATION SH.3

FIGURE 28

ρ_0 (km)



STATION SH.3

PO 1 = 0.100000E 04 Ω m H 1 = 0.410000E-01 km

PO 2 = 0.100000E 01 H 2 = 0.500000E-02

PO 3 = 0.800000E 04 H 3 = 0.900000E 01

PO 4 = 0.150000E 02 H 4 = 0.700000E 01

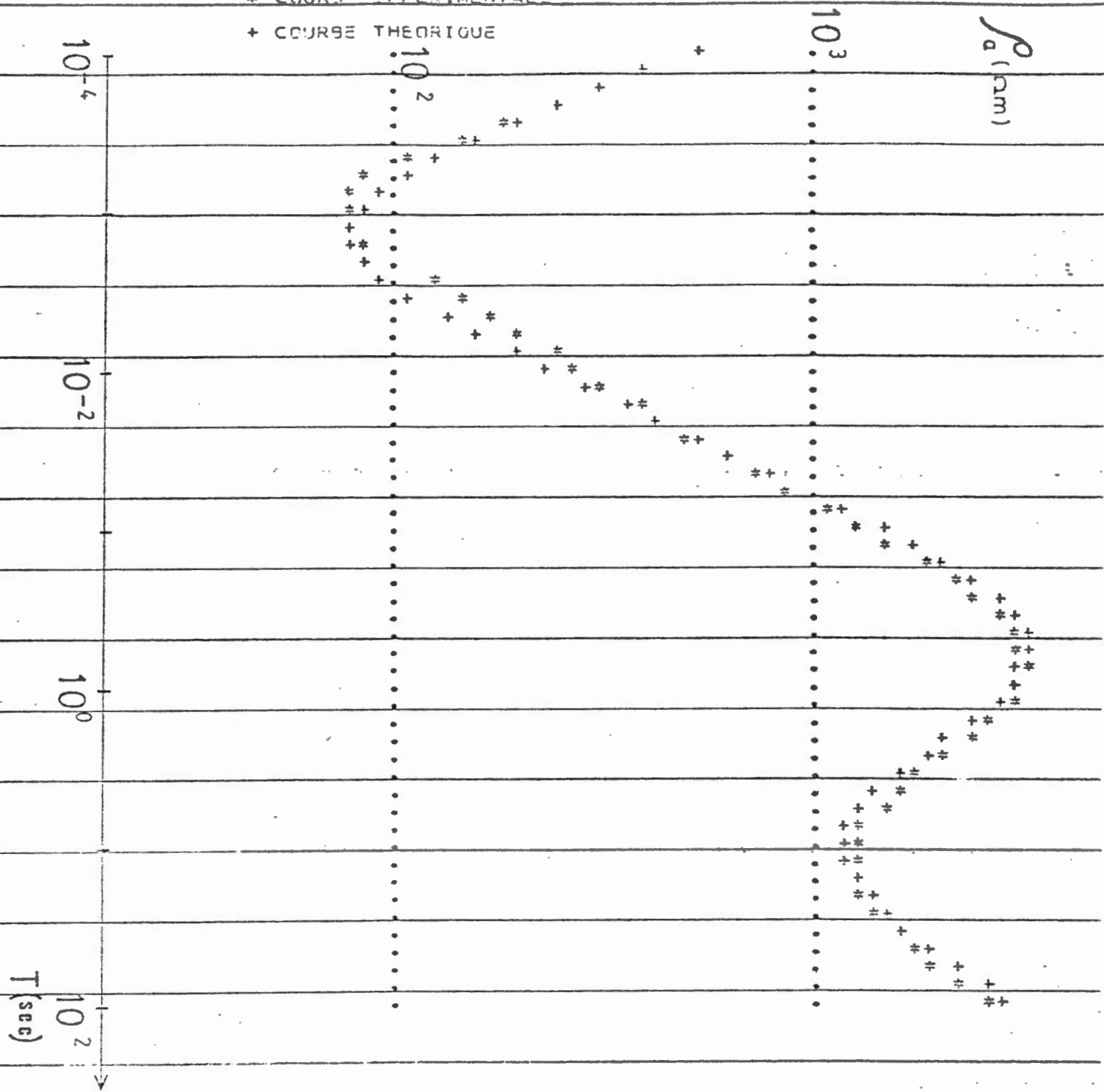
PO 5 = 0.100000E 04 H 5 = ∞

STATION SH.4

FIGURE 29

* COURSE EXPERIMENTALE

+ COURSE THEORIQUE



STATION SH.4

RD 1 = 0.300000E 04 km H 1 = 0.800000E-01 km

RD 2 = 0.240000E 01 H 2 = 0.500000E-02

RD 3 = 0.300000E 04 H 3 = 0.130000E 02

RD 4 = 0.600000E 03 H 4 = 0.250000E 02

RD 5 = 0.100000E 05 H 5 = 0

STATION SH.5

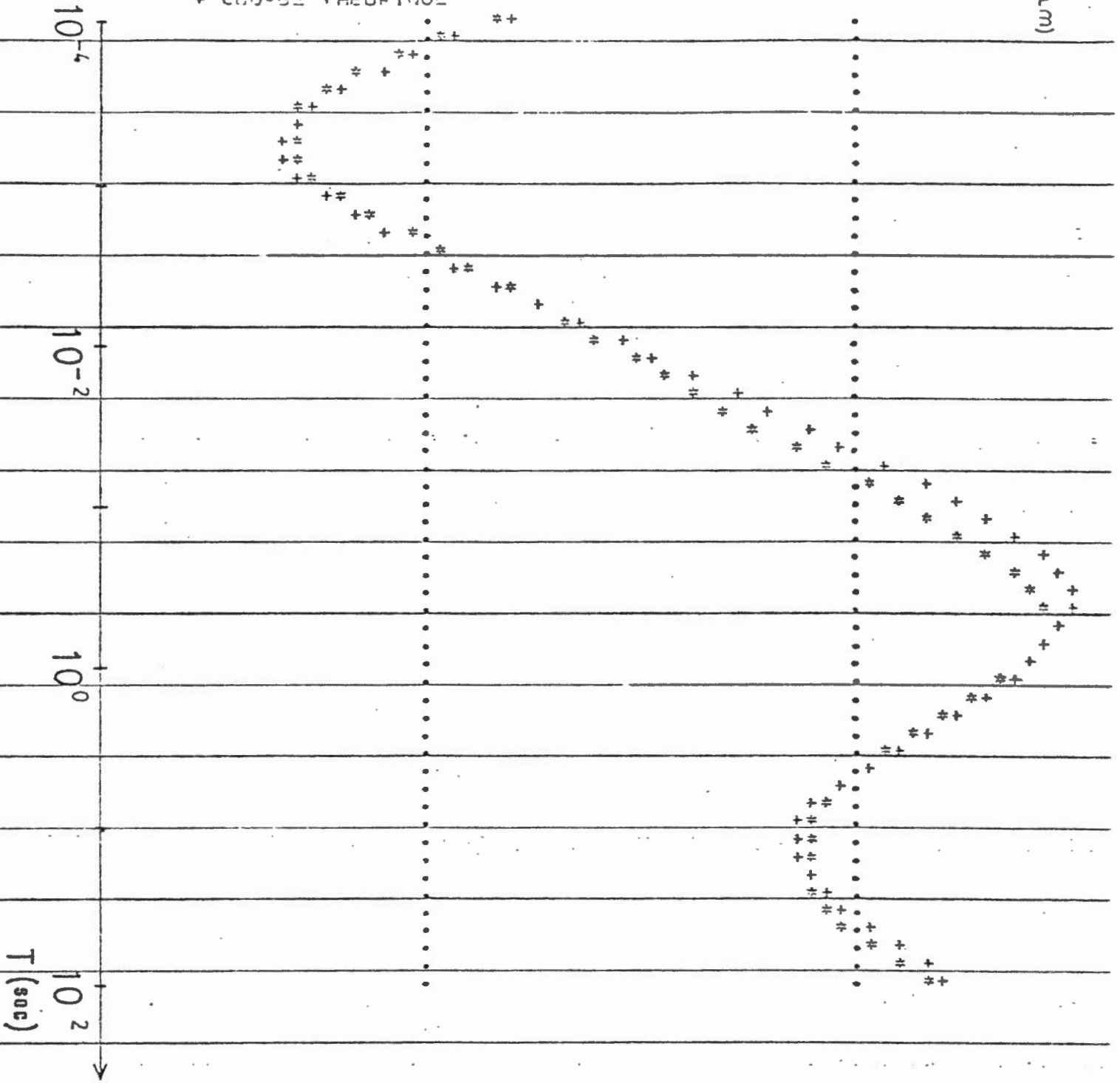
FIGURE 30

10³

ρ_a
(Ωm)

* COURBE EXPERIMENTALE

+ COURBE THEORIQUE



STATION SH.5

PO 1= 0.100000E 04 Ωm H 1= 0.430000E-01 km

PO 2= 0.200000E 01 H 2= 0.500000E-02

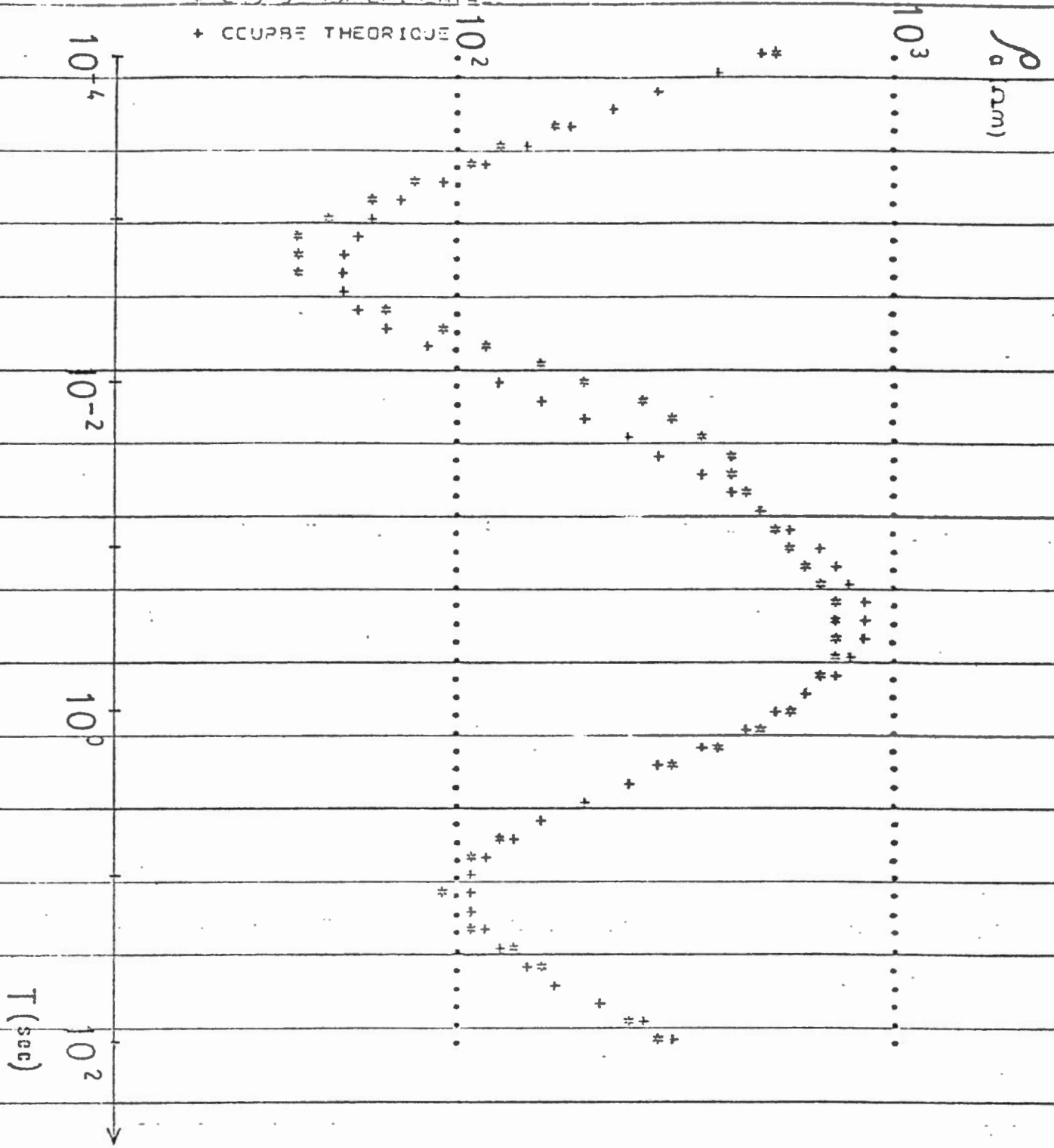
PO 3= 0.800000E 04 H 3= 0.170000E 02

PO 4= 0.350000E 03 H 4= 0.220000E 02

PO 5= 0.100000E 05 H 5= ∞

* COURBE EXPERIMENTALE

+ COURBE THEORIQUE



STATION SR.1

RC 1 = 0.300000E 04 Ω m H 1 = 0.800000E-01 km

RC 2 = 0.800000E 00 H 2 = 0.240000E-02

RC 3 = 0.600000E 04 H 3 = 0.400000E 01

RC 4 = 0.500000E 03 H 4 = 0.400000E 01

RC 5 = 0.300000E 02 H 5 = 0.500000E 01

RC 6 = 0.100000E 05 H 5 = ∞

SONDAGE M.T.

STATION A

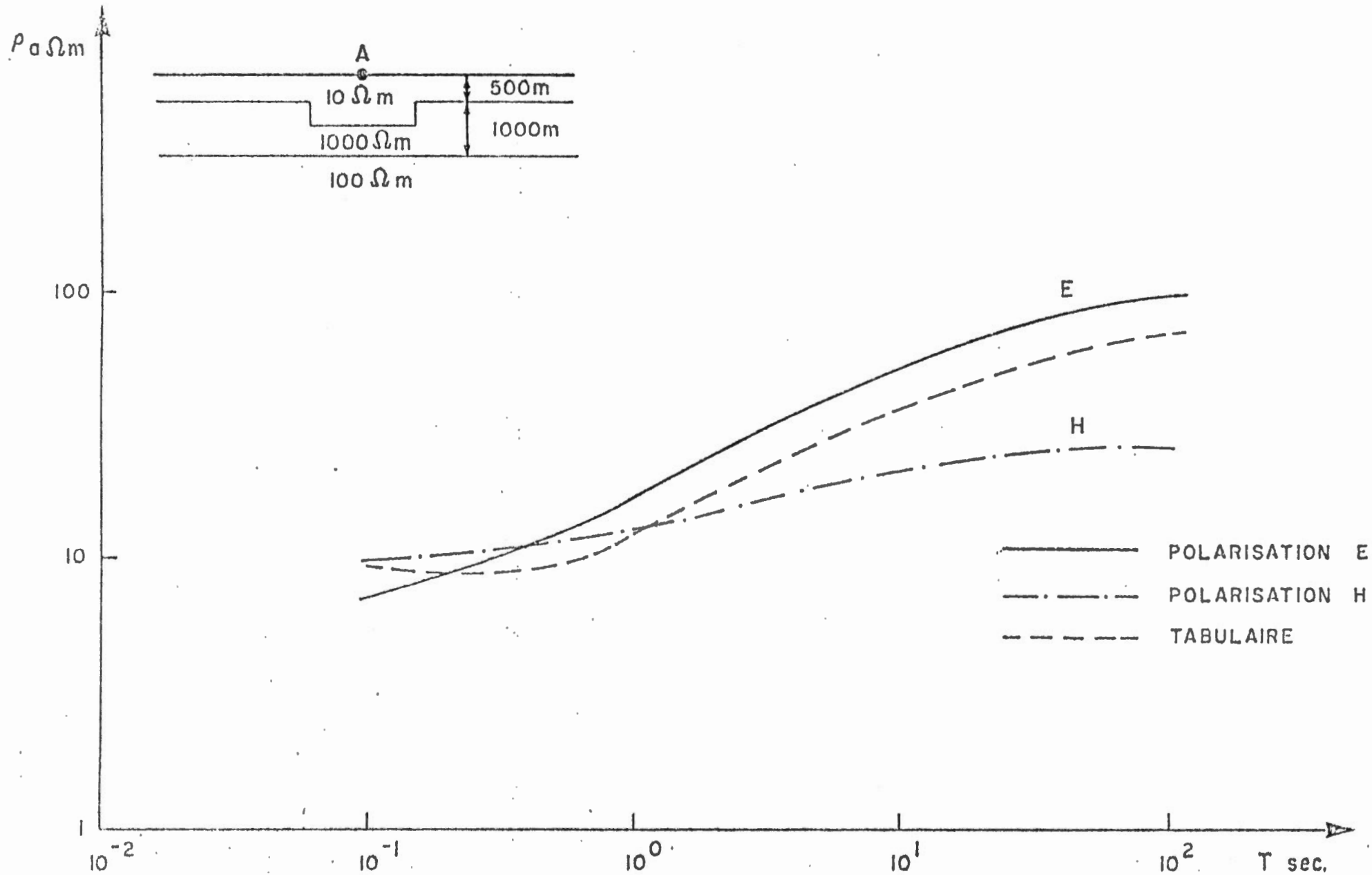
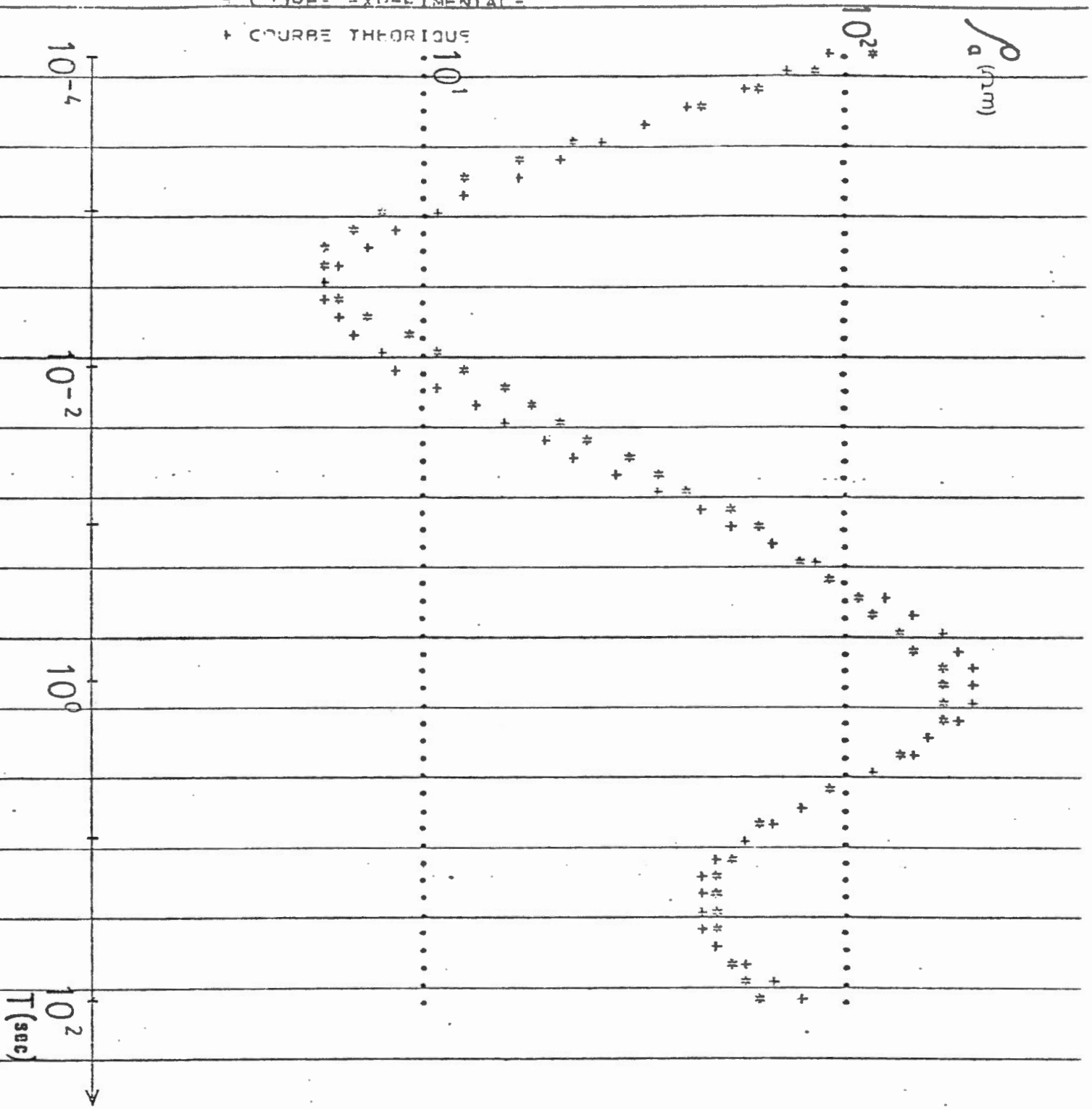


FIGURE 32

+ COURBE EXPERIMENTALE

+ COURBE THEORIQUE



STATION SH.1

RD 1 = 0.500000E 03 Ω_m H 1 = 0.340000E-01 km

RD 2 = 0.330000E 00 H 2 = 0.450000E-02

RD 3 = 0.600000E 03 H 3 = 0.650000E 01

RD 4 = 0.150000E 02 H 4 = 0.500000E 01

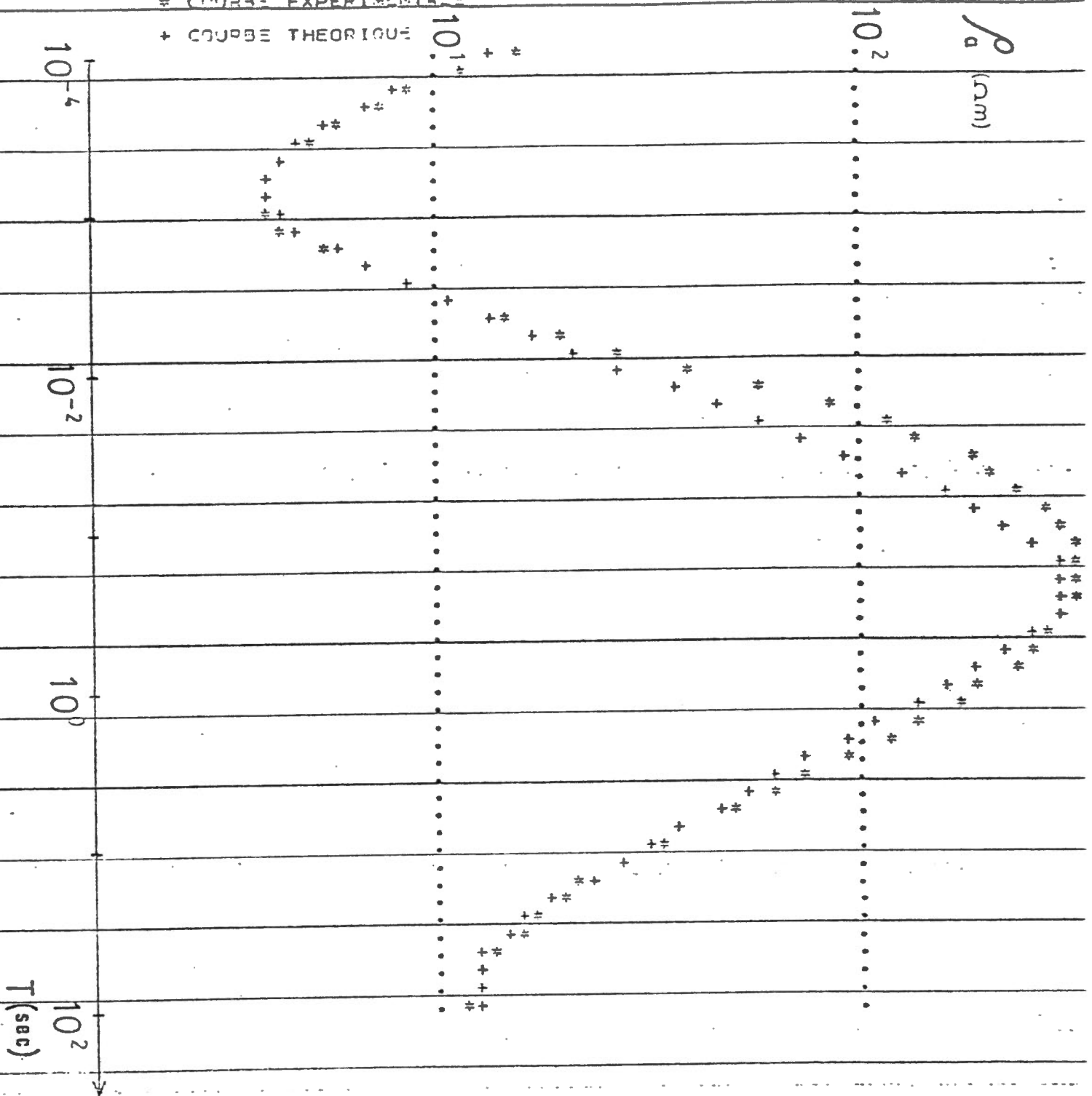
RD 5 = 0.100000E 04 H 5 = ∞

STATION SH.2

FIGURE 34

* COURBE EXPERIMENTALE

+ COURBE THEORIQUE



STATION SH.2

PO 1 = 0.100000E 03 Ω m H 1 = 0.120000E-01 km

PO 2 = 0.350000E 00 H 2 = 0.230000E-02

PO 3 = 0.600000E 04 H 3 = 0.400000E 01

PO 4 = 0.670000E 01 H 4 = 0.300000E 01

PO 5 = 0.100000E 04 H 5 = ∞

FIGURE 35 : COUPE GEOÉLECTRIQUE - PROFIL A
GEOELECTRICAL SECTION - PROFILE A

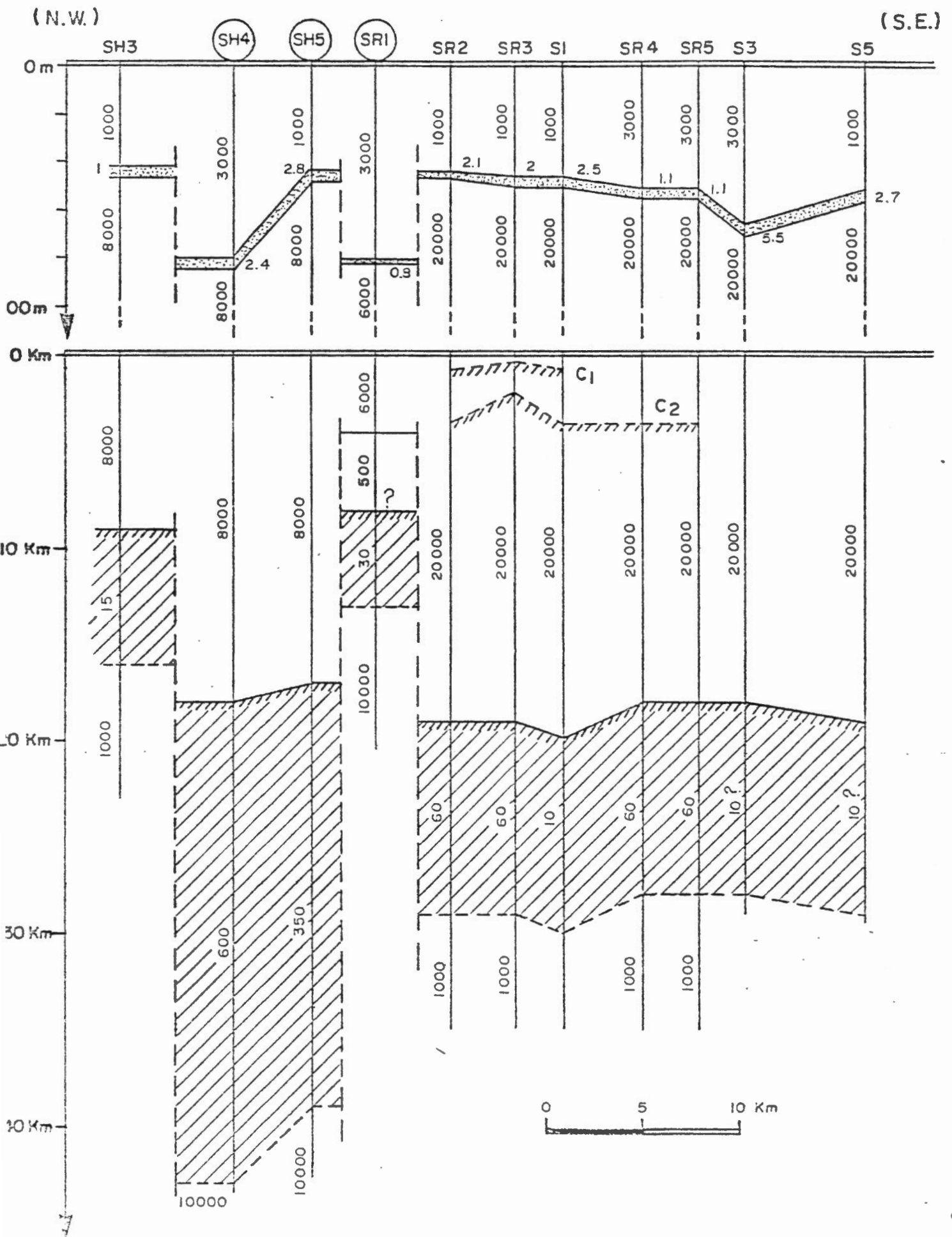
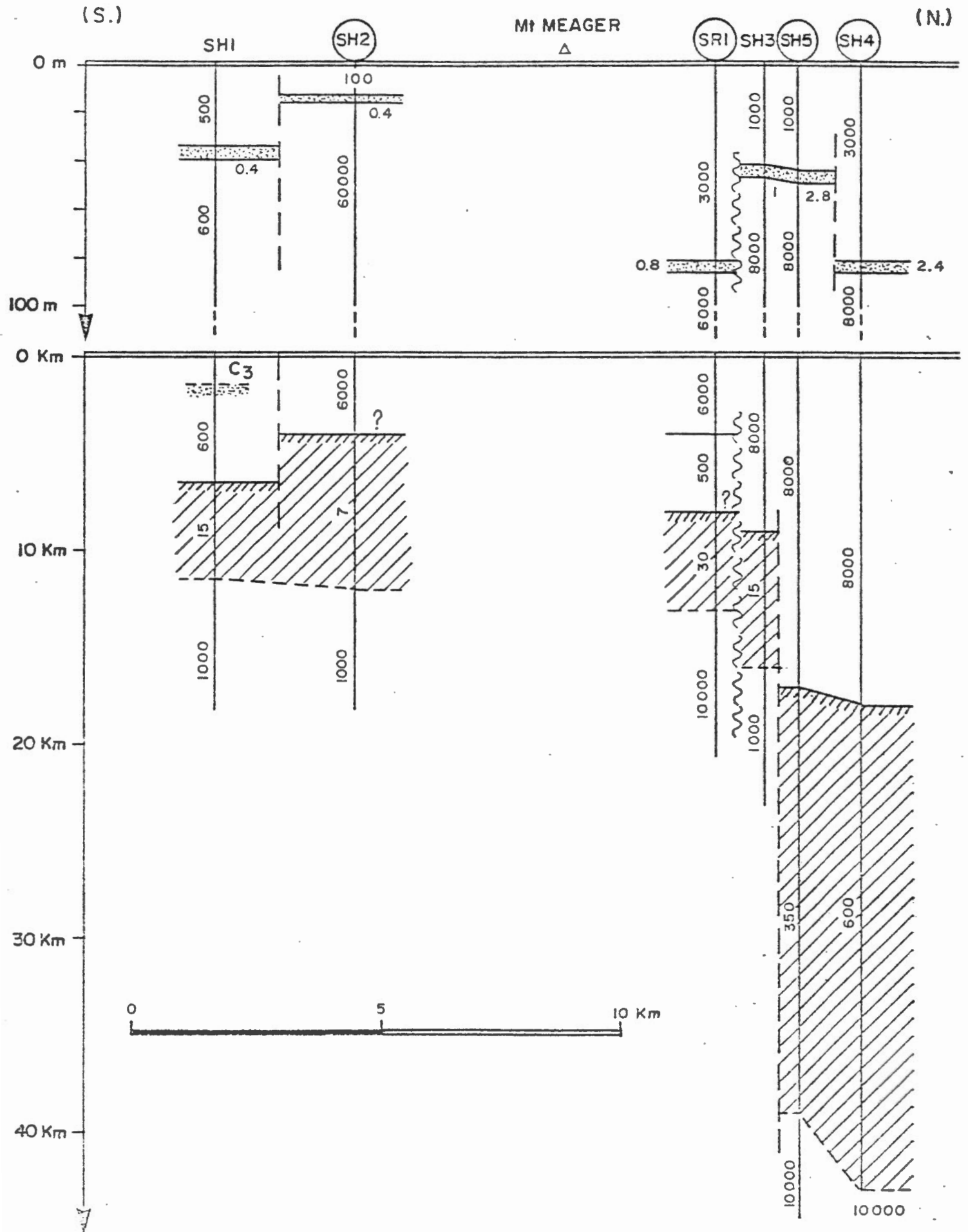
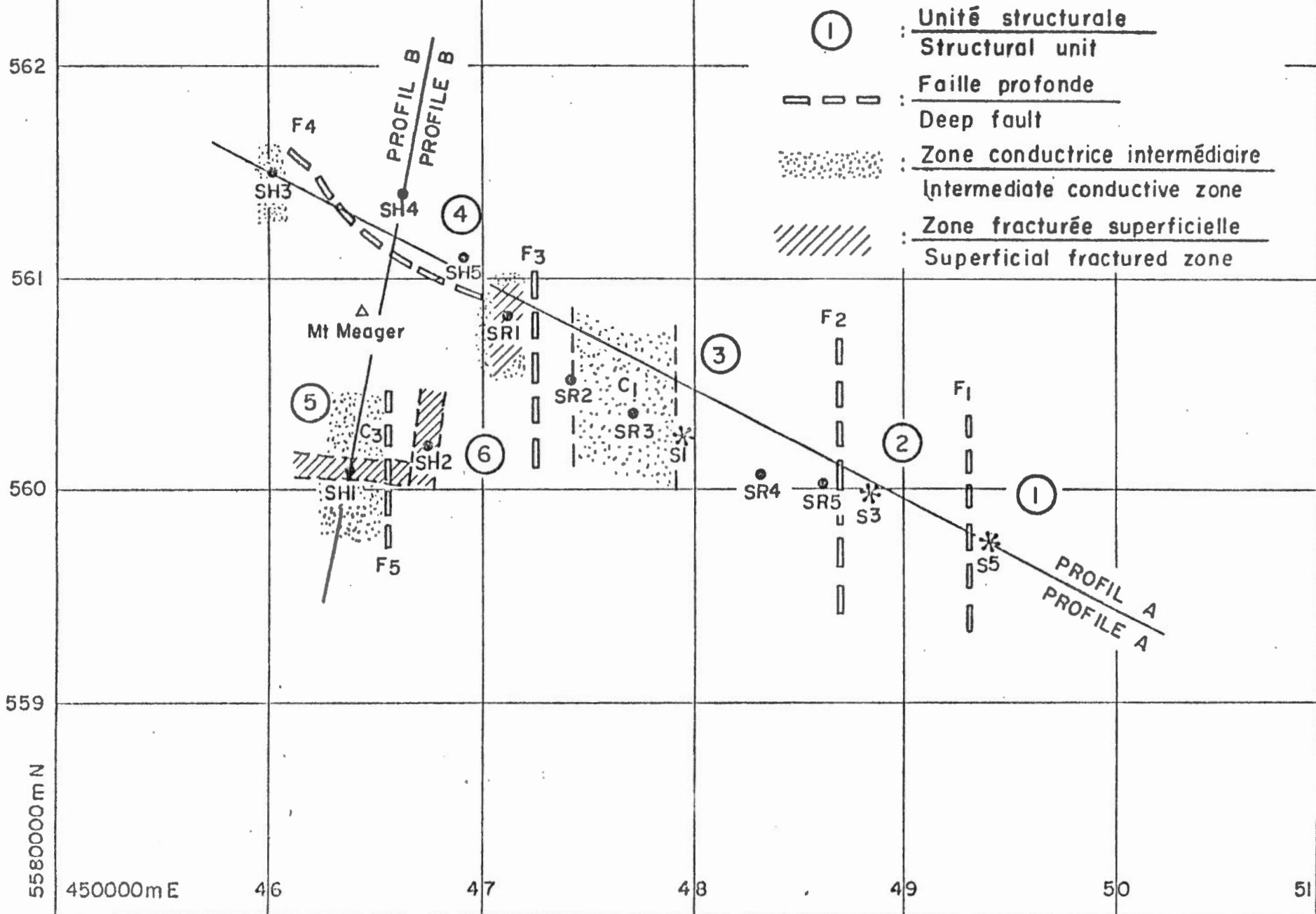


FIGURE 36 : COUPE GEOELECTRIQUE - PROFIL B
 GEOELECTRICAL SECTION - PROFILE B



SYNTHESE GÉNÉRALE DES RESULTATS
 FIGURE 37 : GENERAL SYNTHESIS OF RESULTS



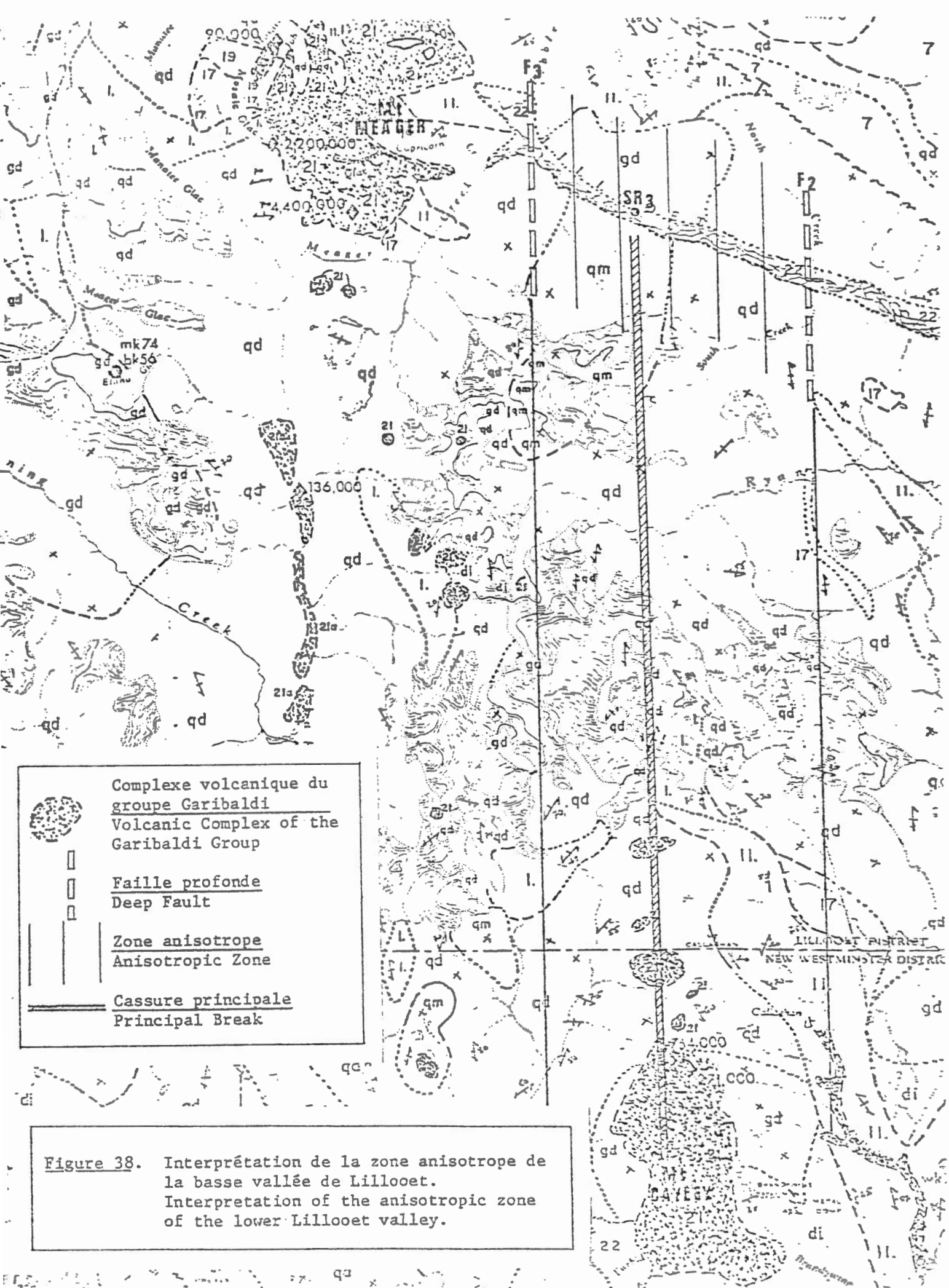


Figure 38. Interprétation de la zone anisotrope de la basse vallée de Lillooet.
 Interpretation of the anisotropic zone of the lower Lillooet valley.